

Job Amenity Shocks and Labor Reallocation^{*}

Sadhika Bagga
Rochester

Lukas Mann
ASU and Minneapolis Fed

Ayşegül Şahin
Princeton and NBER

Giovanni L. Violante
Princeton, CEPR, and NBER

Abstract

We develop an equilibrium model to study the dynamic adjustment of a frictional labor market to aggregate shifts in the demand and supply of a job amenity. When preferences for the amenity are heterogeneous in the population, and its availability is heterogeneous across jobs, labor reallocation ensues. The defining traits of such reallocation (a rise in vacancies and job-to-job transitions, a fall in matching efficiency and in relative wages of jobs supplying the amenity) closely resemble those observed in the post-pandemic U.S. labor market in the aftermath of the shift to remote work. A version of the model calibrated to the U.S. experience matches the data well with shocks of plausible magnitude. Cross-sectional and survey data from various sources offer support for this mechanism.

^{*}We thank seminar participants at Carlos III, CEMFI, Columbia, Cornell, EIEF, Georgetown, IIES Stockholm, LSE, Mannheim, Maryland, Minneapolis Fed, Minnesota, Norges Bank, Northwestern, Notre Dame, Philadelphia Fed, Princeton, PSE, Rochester, Rutgers, St. Louis Fed, Toronto, UCSD, USC, Vanderbilt, Wisconsin, and participants at the conference on Structural Transformation and Macroeconomic Dynamics (Cagliari), workshop on Markets with Frictions (Tinos), Gorman Conference (UCL), Macro Montreal, 2023 SED (Cartagena), 2024 NBER Macro Perspectives for useful comments. We are grateful to Alex Bick and Adam Blandin for their help with the statistics based on the Real-Time Population Survey. First draft: 21 July 2023.

1 Introduction

The notion that workers value both monetary compensation and non-wage job amenities dates back to Adam Smith. In *The Wealth of Nations*, Smith emphasizes that employment choices depend not exclusively on wages, but rather on the *overall advantages and disadvantages* associated with a job. Historically, before the twentieth century, non-pecuniary amenities offered by employers mainly involved ensuring safe and healthy working conditions. As labor markets evolved, jobs began integrating additional benefits such as health insurance and retirement plans. More recently, amenities have further expanded to include workplace facilities –such as cafeterias, gyms, and day-care– as well as flexible schedules and alternative work arrangements in a quest for better work-life balance.

Models of frictional labor markets –which traditionally focused on wages as the sole determinant of job desirability– have increasingly recognized the significance of non-pecuniary amenities in shaping the wage distribution and sorting patterns between workers and firms. However, analyses in this area have typically focused on cross-sectional heterogeneity and long-run comparative statics (see [Mas, 2025](#), for a recent survey).

In this paper, we adopt a novel perspective by blending insights from this literature with business cycle theory to study the short-run labor market adjustment to aggregate shocks that alter the demand and supply of job amenities. Our motivation stems from the peculiar labor market dynamics observed in the U.S. economy following the COVID-19 pandemic. The pandemic served as a large-scale macroeconomic natural experiment that triggered widespread adoption of a relatively new job amenity: work from home.

A few observations illustrate the magnitude of this shift. The share of fully-remote paid working days in the U.S. surged from 6-7% before the pandemic to 28% in 2023, implying that nearly 40% of employees currently have some form of hybrid work arrangement ([Barrero et al., 2023a](#)). Workers who value remote work –roughly half of the labor force– would, on average, accept wage reductions of nearly 8% for the ability to work remotely two days per week ([Barrero et al., 2023b](#)). In the technology sector, this willingness to pay rises to 25% ([Cullen et al., 2025](#)). Survey data indicate that at least one in five job transitions between February 2020 and October 2022 involved a shift from onsite work toward fully or partially remote employment ([Bick and Blandin, 2021](#)). Statistics drawn from LinkedIn job postings in February 2022 reveal that, although remote positions accounted for less than 20% of all paid listings, they attracted over 50% of total job applications.¹ Collectively, these findings indicate that the post-pandemic shift to remote

¹LinkedIn data story titled "In a First, Remote Jobs Attract a Majority of Applications on LinkedIn" by

work had a profound impact on workers' employment trajectories. Additional survey-based evidence (e.g. [Chen et al., 2023](#)) suggests that a demand-side interpretation of the shock (i.e., a change in attitudes toward remote work) has more empirical support than a supply-side one (i.e., a break-through in remote-work technology).²

Turning to aggregate labor market dynamics, we document that, in the aftermath of this shock, the adjustment of the U.S. labor market exhibited some distinctive features compared to previous recoveries, suggesting that an unconventional shock impacted the economy. First, the Beveridge curve exhibited a wide loop and a vertical shift unlike its commonly observed horizontal movements, and the vacancy rate jumped to historically high levels. Second, the monthly quits rate for employed workers reached 3% in 2021, almost 50% more than in 2019, the so-called *Great Resignation*. Third, aggregate matching efficiency (the ratio of hires to contacts) persistently deteriorated, in spite of a tight labor market, leading to a substantial long-lasting drop job-filling rates. Cross-sectional data reveal that the intensity of these patterns varied systematically across sectors in line with each sector's share of teleworkable jobs, as classified by [Dingel and Neiman \(2020\)](#): non-teleworkable sectors experienced the largest increase in vacancies, rise in quits, and drop in job filling rate. In addition, real wages in non-teleworkable occupations increased relative to those in teleworkable ones.

Our hypothesis is that these observed labor market dynamics reflect a post-pandemic shift in worker preferences away from on-site work toward alternative, more flexible remote work arrangements which triggered a reallocation of labor in the economy. In the wake of this aggregate shock, workers quit jobs without the amenity (more so in the non-teleworkable sectors) and move to more attractive positions, driving up job-to-job transitions. These jobs then become idle, leading to rising vacancies (more so in the non-teleworkable sectors). But these vacant jobs are now less desirable and harder to fill, so aggregate match efficiency falls and job filling rates decline (more so in the non-teleworkable sectors). Because most reallocation occurs via direct job-to-job transitions, unemployment remains subdued even as vacancies rise, producing the vertical shift in the Beveridge curve seen in the data. Finally, teleworkable jobs experience larger wage declines, as the growing value of the remote-work amenity gives rise to a negative compensating differential.

A formal and quantitative assessment of this hypothesis requires developing a dynamic equilibrium model of a frictional labor market with the minimal set of ingredients

Greg Lewis, April 7, 2022.

²See also [Sedláček and Shi \(2024\)](#) for a model-based argument in favor of a shift in worker preferences.

needed to confront the data. The core of our model has the same structure as [Lise and Robin \(2017\)](#): random matching with on-the-job search and wage setting which follows a sequential auction protocol. To this building block, we add four key features: (i) idiosyncratic match values which render aggregate matching efficiency endogenous and responsive to shocks; (ii) heterogeneity in jobs' ability to supply non-pecuniary amenities and in workers' valuation of said amenities, which lead to divergent job ranking across workers and re-sorting after the shock; (iii) a costly choice of activating the amenity, for the subset of jobs where it is feasible to do so, which allows ongoing matches to "upgrade" the job; (iv) sunk job creation costs which make vacancies a stock variable whose dynamics are driven by inflows and outflows. As a result, quits induce vacancies.

While our general framework is suitable to studying labor market responses to shocks that shift demand and supply of job amenities, we specialize our application to the post-pandemic dynamics of the U.S. economy. Analyzing this episode requires incorporating two additional aggregate disturbances, besides the job amenity shock: (i) a temporary productivity decline to account for the brief yet severe downturn of 2020; (ii) a rise in the opportunity cost of work –a negative labor supply shock– to capture pandemic-related health concerns, expanded unemployment insurance, and generous fiscal transfers.

After calibrating the steady-state of the model, we use the impulse response functions to infer the realizations of these three shocks that best explain several dimensions of the post-pandemic labor market dynamics. Methodologically, we build on [McKay and Wieland \(2021\)](#) who show how to implement the linear Kalman filter to recover the shocks that generate observed aggregate time series without relying on a state space representation of the model, but only exploiting impulse response functions. We generalize their approach in two dimensions: (i) we use the fully nonlinear model's impulse responses, allowing for size and sign dependence; (ii) we do not rely on exact identification but, because we have more moments to match than shocks, we implement a minimum distance estimator. Once we feed the estimated shock paths in the model, we are able to match our target time series quite well over the three years starting from the onset of the pandemic. Quantitatively, the estimated size of the shift in worker propensity for remote work is equivalent to a growth in compensating wage differential in line with survey evidence.

The model calls for a negative productivity shock to explain the short-lived recession triggered by the lockdown and its swift rebound. Together with a negative labor supply shock, the model can fully capture the unemployment response and the short-run wage dynamics. Overall, the response of the economy following these shocks is quite standard. The novel shock that raises the value workers place on the job amenity, work from home,

is the one that sets off a sustained wave of labor reallocation. A shock decomposition reveals that this is the driving force of the observed rise in job-to-job transitions, the surge in vacancies, the fall in match efficiency, and the decline in compensating wage differential for teleworkable jobs, as conjectured by our hypothesis. The model also shows that this last force exerts downward pressure on real wages, a channel that has found direct empirical support in survey data (Davis, 2024). When we analyze a technology shock that makes upgrading (i.e., allowing for remote work) cheaper on teleworkable jobs, our findings are qualitatively similar, though less pronounced.

Related Literature. Our paper contributes to three main strands of literature. The first is the literature that studies the role of non-wage amenities in frictional environments. The second is the small, but growing, literature that treats vacancies as a stock instead of a flow variable. The third is the more recent, and ongoing, literature that has focused on interpreting post-pandemic macroeconomic dynamics.

The idea of compensating wage differentials for non-pecuniary job attributes, formalized by Rosen (1986) in competitive environments, was incorporated into search models by Hwang et al. (1998). Their main finding was that, in the presence of frictions, the equilibrium relationship between wages and non-wage job characteristics generally bears little resemblance to workers underlying valuations – an insight that informs all empirical estimates of workers marginal willingness to pay for job amenities (e.g. Bonhomme and Jolivet, 2009; Lamadon et al., 2024). Our quantitative analysis indeed confirms that a reduced-form estimate of compensating differentials within the model would differ substantially from workers’ true valuations. Further developments of this literature studied how worker preferences, firm technology and market frictions combine to determine equilibrium job amenities in the context of wage dispersion and gender wage gaps (Albrecht et al., 2018; Le Barbanchon et al., 2021), job search behavior and worker mobility (Hall and Mueller, 2018; Nosal and Rupert, 2007), heterogeneous job ladders and sorting (Lindenlaub and Postel-Vinay, 2023; Sorkin, 2018), for example. Our analysis extends, for the first time, these insights to a framework amenable to the study of aggregate dynamics, and argues that they are instrumental to understand the relation between the sudden pervasive uptake of a job amenity, work from home, and the singularities of the post-pandemic labor market.

One key building block of our frictional model is that vacancies are a stock, not a flow. Because firms incur a sunk cost when creating a new position, unfilled vacancies

retain positive value in equilibrium even under free entry.³ While this approach is standard in firm-dynamics models, it remains rare in search-and-matching frameworks (see e.g., [Fujita and Ramey, 2007](#); [Hornstein et al., 2007](#); [Coles and Kelishomi, 2018](#)), though it has gained traction in light of recent evidence on the prevalence of vacancy chains and replacement hires ([Mercan and Schoefer, 2020](#); [Elsby et al., 2022](#); [Qiu, 2024](#)). Besides being more realistic –and allowing a tighter connection to the notion of job vacancy measured by the JOLTS (Job Openings and Labor Turnover Survey)– this is the crucial feature that allows the model to generate a rise in vacancies caused by a spike in quits, even though the value of those undesirable idle jobs has deteriorated over time. We document that the correlation between quits and vacancies in the post-pandemic recovery is much stronger than in previous ones. Finally, the non-zero value of a vacancy breaks the block-recursivity exploited by [Lise and Robin \(2017\)](#), and makes the computation of aggregate dynamics somewhat more demanding.

Our paper is also closely related to an ongoing literature that studies the evolution of the U.S. labor market after the pandemic. Some papers identified the vacancy-to-unemployment ratio as a key driver of the high and persistent inflation ([Benigno and Eggertsson, 2024](#); [Blanchard and Bernanke, 2023](#)). Others argued that causality runs the other way, i.e. the unexpected inflation surge was the cause of unusually strong market tightness. The underlying hypothesis here is that the erosion of real wages for incumbents incentivizes search for new jobs, where nominal wage contracts of new hires are more responsive to inflation ([Pilossoff and Ryngaert, 2024](#); [Guerreiro et al., 2024](#)). [Afrouzi et al. \(2024\)](#) develop this insight in an equilibrium search model and show that it can generate the observed increase in job-to-job quits and vacancies. Relative to this literature, we focus on the decline in job values associated with the absence of a remote work option as the trigger for on-the-job search. Both of these channels have empirical support in the data and emerge as the leading explanations for post-pandemic labor market dynamics by potentially reinforcing each other. Finally, our paper contributes to the literature on the inflation-reallocation trade-off in the job ladder ([Moscarini and Postel-Vinay, 2023](#)), showing that labor reallocation driven by the spread of remote work has helped to temper wage growth.

The rest of the paper is organized as follows. Section 2 introduces the different data sources we use in the paper and illustrates the key stylized facts of the post-pandemic la-

³For example, creating an additional job at a call center requires purchasing a chair, a desk, and the necessary equipment. If a worker quits the job and that match is dissolved, rehiring a new worker does not require making the initial investment again.

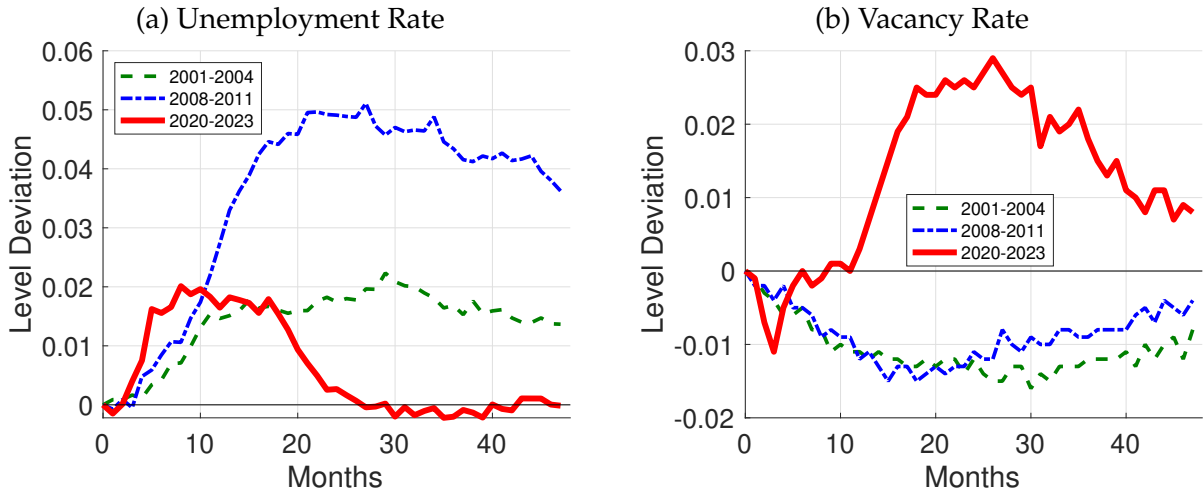


Figure 1: Level deviation in the unemployment rate (left) and log deviation in the vacancy rate (right) for 2001-2004, 2008-2011, and 2020-2023.

Notes: CPS, JOLTS, and authors' calculations. The values are normalized to zero for January 2001, 2008, and 2020.

bor market recovery. Section 3 presents the theoretical framework. Section 4 describes the model's parameterization. Section 5 presents the impulse response functions of the three aggregate shocks, and the methodology to estimate shocks. Section 6 shows the model's fit of the data, the shock decomposition, and additional results. Section 7 concludes the paper.

2 The Post-Pandemic Labor Market in the U.S.

In this section we begin by documenting that –along a number of key dimensions– the U.S. aggregate labor market dynamics after the pandemic have been distinctive, especially when compared to previous recoveries. We then present existing survey-based evidence suggesting that the pandemic prompted a shift in workers' attitudes toward a key job amenity, the opportunity to work from home. Next, we present further observations which support the idea that this amenity valuation shock triggered a process of labor reallocation that can account for the post-pandemic aggregate and sectoral labor market dynamics.

2.1 The Aggregate Labor Market

In this section we discuss the evolution of key labor market indicators after the onset of the pandemic and compare them with earlier recoveries.

2.1.1 Unemployment and Vacancies

The pandemic caused an unprecedented disruption in the U.S. labor market: payroll employment decreased by 14.4%, the unemployment rate rose by 11.2 percentage points, and job vacancies dropped by 34% in the short time span from February to April 2020. Once lockdowns and other restrictions were lifted, however, the labor market exhibited a remarkably quick recovery compared to previous recessions. Within two years, the unemployment rate retreated to its lowest post-war level of 3.5% and job openings reached their highest peak in the last two decades.

A unique feature of the pandemic was the record-high number of workers who were put on temporary layoffs because of widespread mandatory business closures. These "workers with jobs but without pay" accounted for 80% of the surge in unemployment but were almost entirely reabsorbed into employment by the end of 2020 ([Hall and Kudlyak, 2022](#)). Motivated by these observations, we exclude unemployed workers on temporary layoffs from the unemployment stock and treat them as non-participants. After this adjustment, the peak of the "strictly jobless" unemployment rate was only 4.9% in November 2020. For consistency, we also exclude recalls from hires, and temporary layoffs from separations.⁴

Figure 1 compares the evolution of the unemployment rate and the vacancy rate for the last three recessions. Each series is normalized to zero at the beginning of the corresponding recession. The pandemic recession stands out in its briefness. Not only did the unemployment rate peak earlier in the recent cycle, but it also dropped precipitously. The behavior of vacancies has also been very different. The vacancy rate reversed its drop quickly and reached staggering levels, more than 50 percent higher than its pre-pandemic level.⁵ This rapid rebound contrasts sharply with earlier episodes, particularly the recovery from the Great Recession, when the unemployment and vacancy rates did not recover back to their pre-recession levels for almost a decade.

Figure 2 shows the relative behavior of unemployment and vacancy rates in the Bev-

⁴See Figure C1 for a comparison of unemployment rates with and without temporary layoffs.

⁵Figure C2 in the Appendix shows how the traditional measure of labor market tightness, the vacancy-to-unemployment ratio, evolved during the pandemic recession relative to earlier business cycles.

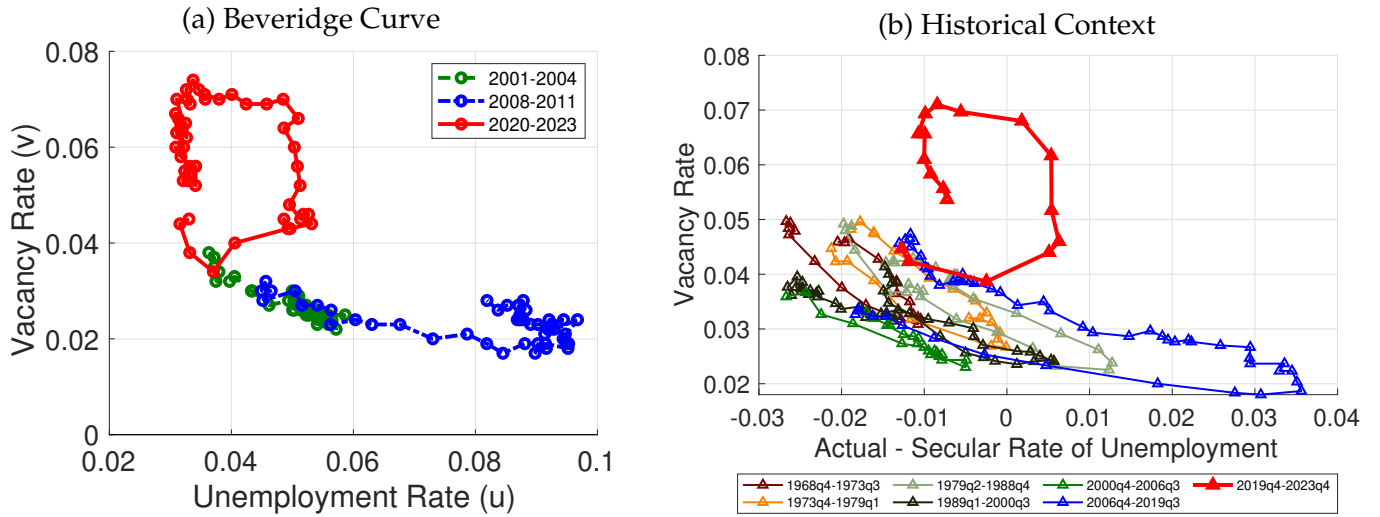


Figure 2: Beveridge Curve over the last three cycles (left) and in historical context (right).

Notes: CPS, JOLTS, and authors' calculations based on [Barnichon \(2010\)](#), [Petrosky-Nadeau and Zhang \(2021\)](#) and [Crump et al. \(2019\)](#)

eridge space. The left panel plots the Beveridge curve for the recoveries in the last 25 years. The most recent loop in the Beveridge curve stands in stark contrast to the ones traced around the last two business cycles both in size and in shape. The loop is much wider and it exhibits a clear vertical pattern. The right-panel of Figure 2 illustrates that the nature of the Beveridge loop after the pandemic remains unprecedented even in comparison to the last 50 years.⁶ From 1968 to 2019, there is a robust negative correlation between vacancies and unemployment: when the unemployment rate exceeded its secular trend, the vacancy rate fell. This robust negative relationship broke down during the pandemic as the unparalleled surge in vacancies induced a far more vertical shift in the Beveridge space.⁷ In addition, we note that –at least in terms of gap between actual and secular unemployment– the U.S. labor market reached the same, and even higher, levels of "tightness" several times in the past 50 years and none of these episodes corresponded to vacancy rates as high as the most recent ones.

⁶We utilize the vacancy series constructed by [Barnichon \(2010\)](#) and [Petrosky-Nadeau and Zhang \(2021\)](#) to extend the vacancy series prior to 2001 (when the JOLTS started). We take into account secular trends in the unemployment rate by comparing the vacancy rate to deviations of unemployment from its secular trend estimated by [Crump et al. \(2019\)](#).

⁷After the Great Recession, a large literature investigated the role of mismatch, unemployment insurance benefits, recruiting intensity, and job search effort to account for the 'large' shift in the Beveridge curve ([Daly et al., 2012](#); [Davis et al., 2013](#); [Hall and Schulhofer-Wohl, 2018](#); [Sahin et al., 2014](#); [Gavazza et al., 2018](#); [Mukoyama et al., 2018](#)). The right panel of Figure 2 shows that, up to that point, that shift was in fact the largest one on record, but it is dwarfed by the most recent one.

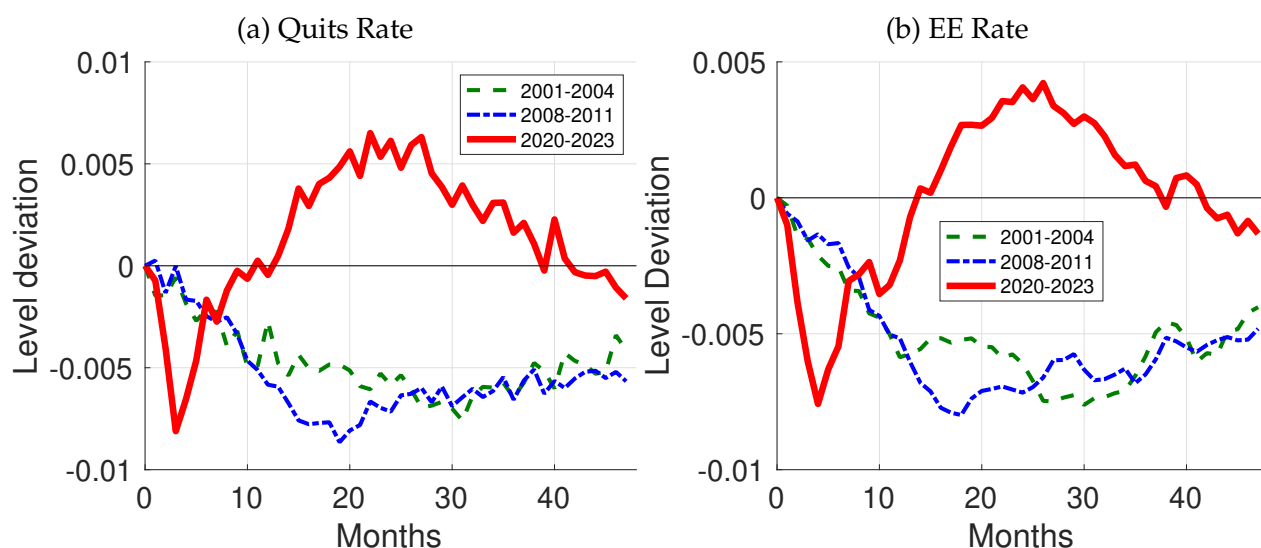


Figure 3: Level deviation in the quits rate (left) and job-to-job transition rate (right) for 2001-2004, 2008-2011, and 2020-2023 periods.

Notes: CPS, JOLTS, and authors' calculations. The values are normalized to zero for January 2001, 2008, and 2020. The quits rate is expressed as JOLTS quits divided by employment. The EE rate is expressed as a 3-month centered moving average of hires from employment divided by employment. EE hires have been constructed to reflect CPS levels and JOLTS cyclicalities as described in Appendix A.

2.1.2 Quits and Job-to-Job Transitions

The second unique feature of this recovery was the so-called *Great Resignation*. Following the end of the acute phase of the pandemic, quits rebounded briskly and reached their highest level since the inception of the JOLTS series, as shown in the left panel of Figure 3. The right panel shows that the surge in job-to-job (EE) transitions was a key component of this surge in quits. Quits behaved very differently from the last two recoveries, as clear from these two panels.

Figure 4 reinforces this point by plotting the quits rate against the deviations between actual and secular rates of unemployment. While both previous cycles exhibited a strong negative relationship between quits and unemployment rate –in the same vein as what was observed for the Beveridge curve– this last episode saw a breakdown of this relationship, and exhibited a pronounced vertical jump in quits.

2.1.3 Job Finding and Job Filling Rates, and Matching Efficiency

The third peculiar fact that characterizes this recovery is a depressed labor market matching efficiency, i.e. the rate at which contacts between idle positions and job seekers trans-

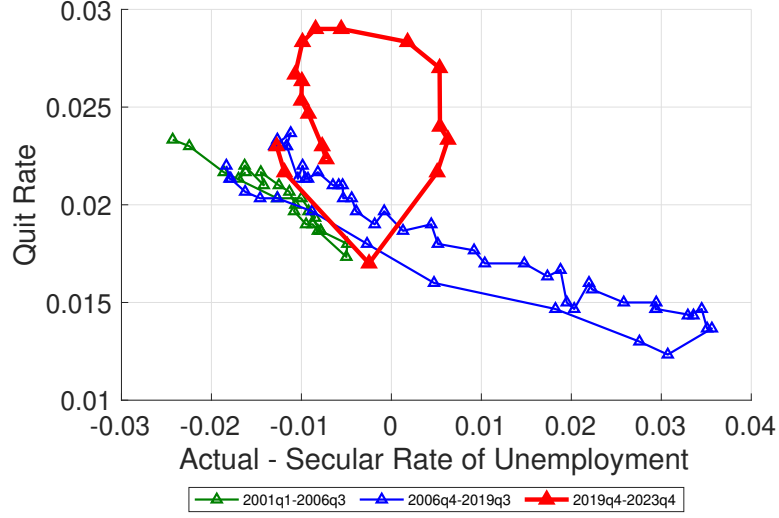


Figure 4: Quits rate and deviation of actual and secular rates of unemployment.

Notes: CPS, JOLTS, and authors' calculations.

late into new job matches.

It is useful to begin by describing the dynamics of job finding and job filling rates over this period since matching efficiency affects both job finding and job filling in the labor market. Figure 5 shows the job finding rate for unemployed job seekers (defined as hires from unemployment divided by the number of unemployed workers) and the job filling rate (defined as hires from unemployment and employment divided by vacancies).⁸ Both series, again, exhibit different dynamics from the last two cycles. The job finding rate, which remained below trend for many years after the 2001 and 2007-2009 recessions, rebounded rapidly after the pandemic but did not exceed its pre-pandemic level.⁹ The job filling-rate remained depressed because of the quick and steep rise in vacancies. However, its decline is larger than one would have expected based on the fact that vacancies surged by over 50%. These observations suggest that the increase in hires was dampened by low aggregate matching efficiency reducing both the job finding and job filling rates.

Measuring aggregate match efficiency requires a minimal structure. We posit that total hires are given by a Cobb-Douglas aggregate matching function (as in our model of Section 3):

$$h_t = h_t^u + h_t^e = A_t v_t^\alpha (u_t + se_t)^{1-\alpha} \quad (1)$$

⁸To be consistent with the model of Section 3, throughout our analysis we abstract from hires from nonparticipation.

⁹The job finding rate for all job-seekers including those from unemployment *and* employment rises only slightly above trend, see Figure C3 in the Appendix.

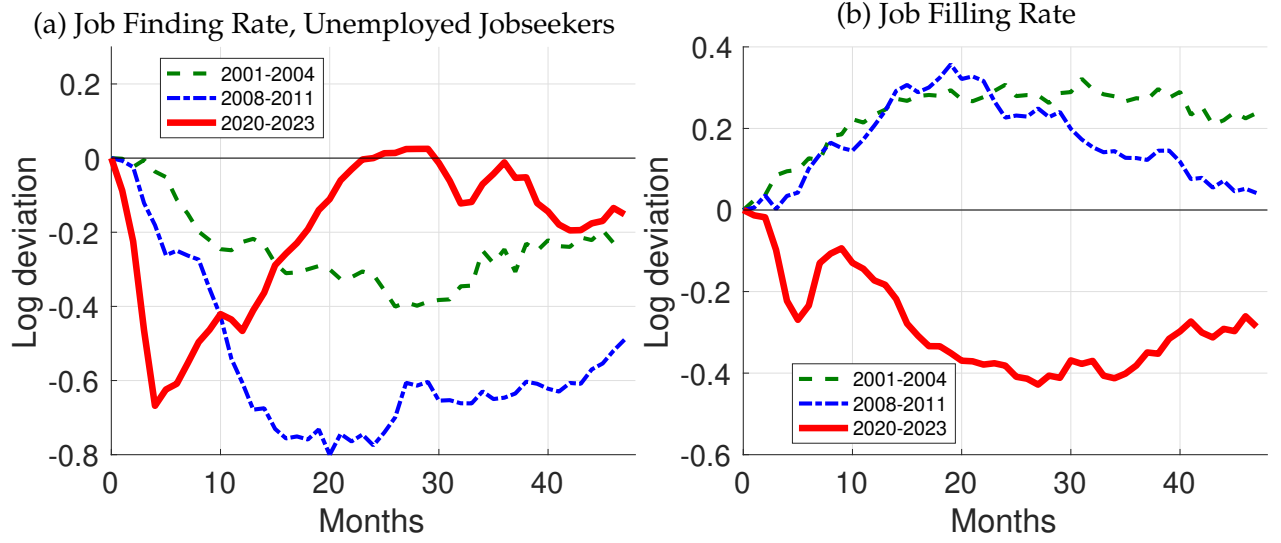


Figure 5: Job finding (left) and job filling rates (right).

Notes: CPS, JOLTS, and authors' calculations. The values are normalized to zero for January 2001, 2008, and 2020. The job finding rate is defined as total hires from unemployment divided by unemployed jobseekers. The job filling rate is defined as total hires from employment and unemployment divided by vacancies. Total hires have been constructed to reflect CPS levels and for JOLTS cyclicalities as described in Appendix A. All series are expressed as a 3-month centered moving average.

where h_t^u are hires from unemployment, h_t^e are hires from employment, v_t are the vacancies posted by firms looking to hire, u_t are unemployed workers and e_t are employed workers. The parameter s denotes the relative search effort of employed job-seekers (with the effort of the unemployed normalized to 1). Finally, A_t is the aggregate matching efficiency parameter. Let $UE_t = h_t^u / u_t$ and $EE_t = h_t^e / e_t$. We can then define the matching efficiency for the unemployed and employed workers separately, using their corresponding job finding rates as

$$A_t^u = \frac{UE_t}{\left(\frac{v_t}{u_t + se_t}\right)^\alpha} \quad \text{and} \quad A_t^e = \frac{EE_t}{s \left(\frac{v_t}{u_t + se_t}\right)^\alpha} \quad (2)$$

Note that these variables are the ratios between matches formed and contacts.¹⁰ We set $\alpha = 0.5$ following Petrongolo and Pissarides (2001). The relative search effort of the employed, s is set to 0.78, which is consistent with our model calibrated in Section 4 and

¹⁰Aggregate matching efficiency is the weighted average of matching efficiency of the unemployed and employed workers where the weights correspond to their relative search input: $A_t = \left(\frac{u_t}{u_t + se_t}\right) A_t^u + \left(\frac{se_t}{u_t + se_t}\right) A_t^e$.



Figure 6: Matching efficiency of the unemployed (left) and employed (right) searchers.

Notes: CPS, JOLTS, and authors' calculations. The values are normalized to zero for January 2001, 2008, and 2020. The matching efficiency of the unemployed and employed are derived in Equation 2 and expressed as 3-month centered moving averages. Hires from unemployment and employment are constructed to reflect CPS levels and JOLTS cyclicalities as described in Appendix A.

close to the value estimated by Faberman et al. (2022).¹¹

Matching efficiency for unemployed and employed job-seekers is shown in Figure 6. Both panels confirm that aggregate match efficiency remained depressed during the recovery from the pandemic recession. Note that these are the only time series that behave similarly to their counterparts over the last two business cycles.

Taking stock. The post-pandemic labor market exhibited three peculiarities: a wide vertical loop in the Beveridge curve caused by a surge in vacancies without a notable change in the unemployment rate, a historically high quits rate –as well as robust worker flows between jobs– and depressed aggregate matching efficiency. These three facts indicate that one cannot simply resort to an exceptionally tight labor market as an explanation. A hot labor market –where productivity and/or labor demand is very strong– would induce a sharply negative correlation between unemployment and vacancies and, above all, would strengthen match efficiency. The data do not support this view.¹²

Instead, a fundamentally different type of aggregate shock is required to explain these

¹¹Most alternative values of s leave the qualitative properties of match efficiency unchanged.

¹²See also Gittleman (2022) for evidence that the pace of job quits has risen more quickly than one would have expected from labor market tightening alone.

dynamics. We hypothesize that this shock is related to the radical change in the nature of work arrangements brought on by the pandemic. Specifically, we think of this aggregate shock as a shift in workers’ preferences toward the work-from-home amenity, which in turn prompted a reallocation of labor. In the next two sections, we first document the changes in prevalence of remote work and offer some evidence on the post-pandemic shift in attitudes toward remote work. We then show some key empirical patterns in support of our mechanism.

2.2 The Shift in Workers’ Attitudes Toward Work-From-Home

The pandemic triggered a dramatic shift to work-from-home which settled at a much higher level compared to its prevalence before the pandemic: In 2019, full work-from-home days accounted for just 7% of all paid workdays, compared to 30% in 2023 (Barrero et al., 2023a, Figure 1).¹³ This transition to remote work, however, occurred unevenly across occupations. Dingel and Neiman (2020) assessed the feasibility of remote work at the onset of the pandemic for detailed occupational categories based on their task content. According to their classification, in 2020 roughly 63% of the workers were employed in non-teleworkable occupations —jobs that must be performed on site due to technological limitations— while the remaining 37% held jobs amenable to teleworking.

Figure 7 combines the Dingel-Neiman taxonomy with CPS data on employees’ work arrangements and shows how the share of employees working from home changed over time across occupations measured at the 5-digit level.¹⁴ We rank 5-digit SOC occupations by their share of employees working from home in February 2020 (left panel) and Oct 2022-Dec 2023 (right panel) and color code each occupation based on the Dingel-Neiman teleworkability classification: red bars represent occupations in which telework is feasible (e.g., telemarketers and managers), while blue bars represent occupations where telework is less feasible (e.g., dentists and firefighters).¹⁵ Comparison of the left and right pan-

¹³We reproduce statistics from Barrero et al. (2021) in Figure C4 in the Appendix. The figure plots the full work-from-home days as a fraction of all paid days (green solid line), and the share of workers in hybrid work arrangements (blue dashed line) from the Survey of Working Arrangements and Attitudes. Both series remained persistently high between 25-30% from 2022 until the most recent sample period in March 2025.

¹⁴The Bureau of Labor Statistics (BLS) added new questions to the CPS starting in October 2022 that ask whether people had teleworked or worked at home for pay in the survey reference week. The employed respondents were also asked if they had teleworked in February 2020.

¹⁵Dingel-Neiman classify about 950 ONET occupations as either teleworkable (1) or non-teleworkable (0). Using their taxonomy, we compute employment-weighted average teleworkability of 423 CPS occupation codes at the SOC 5-digit level, which is continuous on the interval $[0, 1]$.

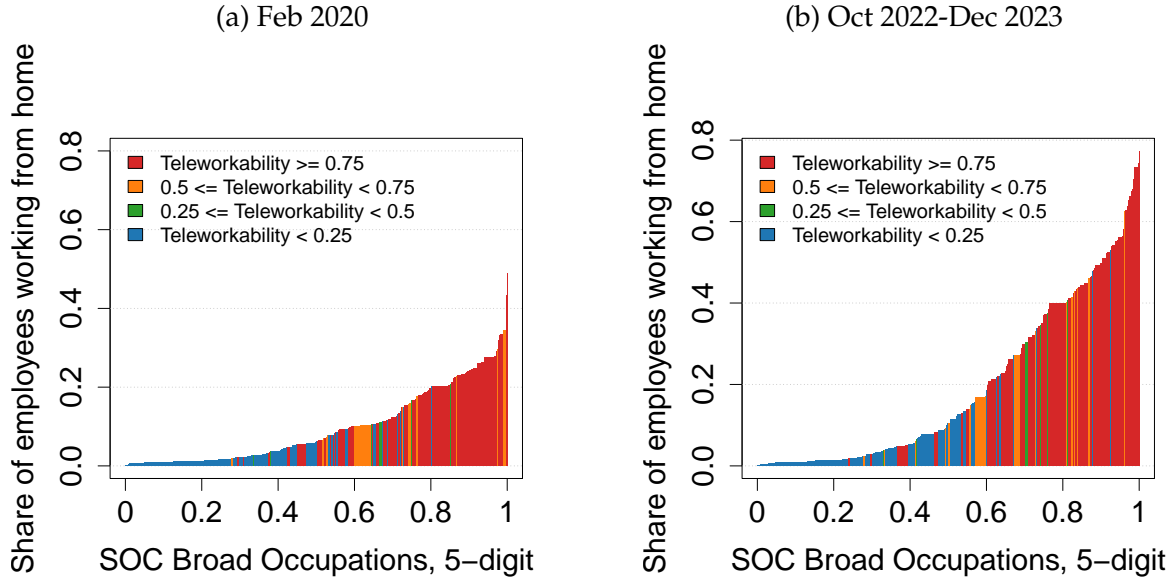


Figure 7: Feasibility of teleworkability and share of employees working from home across occupations.

Notes: CPS, and authors' calculations. We rank 423 occupations at the SOC 2010 5-digit level by their share of weekly hours spent teleworking, shown on the y-axis, from the CPS Telework supplement (October 2022-December 2023). Width of the bars indicate employment share of occupations, and the cumulative employment share is denoted on the x-axis. The different colors indicate the share of teleworkable jobs in an occupation based on tasks performed from [Dingel and Neiman \(2020\)](#).

els show that after the onset of the pandemic there was widespread adoption of remote work arrangements, but only in those occupations where teleworkability was feasible. Furthermore, the x-axis shows the cumulative employment share of teleworkable and non-teleworkable jobs, which remained nearly steady over the two periods.

This permanent shift in work arrangements was not the result of a major technological breakthrough: the infrastructure and technology that allowed WFH were largely in place prior to the pandemic, but utilization rate was low.¹⁶ We argue instead that a major driver of this transformation was the change in workers' preferences toward WFH. Two independent surveys, the Survey of Working Arrangements and Attitudes (SWAA) and Survey of Consumer Expectations (SCE), provide evidence that WFH has become an important amenity for workers after 2020.

The Survey of Working Arrangements and Attitudes (SWAA), administered by [Barro et al. \(2021\)](#) to over 30,000 respondents since May 2020 contains two relevant questions. The first one is: *Compared to your expectations before COVID (in 2019) how has working*

¹⁶See [Bai et al. \(2021\)](#) for a discussion of the technological advances before the pandemic that already made work from home feasible.

from home turned out for you?. 60% of individuals responded "better/substantially better/hugely better than expected". The second one is: *Since the COVID pandemic began, how have perceptions about working from home (WFH) changed among people you know?.* Nearly 2/3 responded "improved among some/improved among most/improved among all".¹⁷ Moreover, respondents who value WFH were willing to accept pay cuts around 8% on average in exchange for working from home 2-3 days a week. One potential reason is jobs with remote work arrangements enable workers to have greater flexibility and more time for home production and leisure activities.¹⁸

The specially-tailored survey of participants drawn from the Survey of Consumer Expectations designed by [Chen et al. \(2023\)](#) also concludes that the pandemic increased the desired share of hours worked from home. In addition, the survey asks whether *WFH is now more important for respondents' job choice*. More than half of the October 2021 respondents reported that the availability of working remotely was now more important to them when choosing a job, while the remaining share was largely indifferent.

In addition to these surveys, the Real-Time Population Survey (RPS), using retrospective questions documented that between February 2020 and October 2022 at least one in five workers who changed jobs transitioned to fully or partially remote work arrangements.¹⁹

Consistent with this evidence, in the rest of the paper we take the view that the source of the aggregate shock was a shift in worker preferences toward jobs that offer the remote-work option, and that many firms adapted to this shift by offering this specific non-pecuniary amenity. In Section 6, we also entertain the alternative view that workers' preferences were stable but the cost to firms of allowing WFH fell over time, and compare and contrast the model's implications.

2.3 Sectoral Labor Market Dynamics by Teleworkability

We next show that the variation in sectoral labor market outcomes provides support to our mechanism. To examine sectoral outcomes, we first compute the share of employment in teleworkable occupations –again using the classification developed by [Dingel and Neiman \(2020\)](#)– across the fifteen two-digit industries in the JOLTS data. The degree of teleworkability varies substantially across sectors: in Technology and Information, Ed-

¹⁷Those with negative perceptions were only 14% and 7%, respectively, for the first and second question.

¹⁸For example, according to the same survey, when employees work from home, they save an average 65 minutes per day by not commuting and taking less time to get ready for work.

¹⁹For details of the survey see <https://sites.google.com/view/covid-rps>.



Figure 8: Labor Market Outcomes by Industry Teleworkability

Notes: CES, CPS, JOLTS and authors' calculations. The x-axis plots the share of teleworkable jobs using [Dingel and Neiman \(2020\)](#) classification aggregated to JOLTS 2-digit industry level. The y-axis plots log deviations of the centered-moving average for each outcome in January 2022 from January 2020. The fitted line is weighted by the centered-moving average of sectoral vacancy shares in January 2020 (also reflected by the size of each circle).

education, and Finance, approximately 70% of jobs are amenable to remote work, whereas in sectors such as Construction, Accommodation, and Transportation, fewer than 20% of jobs can be performed remotely.

Figure 8 shows the change in key labor market indicators from January 2020 to January 2022 across these industries, ranked in ascending order based on the share of teleworkable jobs.²⁰ As the figure shows, sectors with lower shares of teleworkable jobs experienced a larger increase in their vacancy rate (panel a), a sharper drop in the job filling rate (panel b), a more pronounced increase in the quits rate (panel c), and a larger increase (or a

²⁰We implement this analysis at the sectoral level, rather than at the occupational level since JOLTS do not provide information at the occupation level. We focus on the January 2020 to January 2022 period as month 25 from our starting date corresponds approximately to the largest change for virtually all labor market variables we analyzed. We plot 3-month centered moving averages of the data.

smaller drop) in the real wage (panel d) relative to sectors with more teleworkable jobs.

These patterns are consistent with a shift in worker preferences away from on-site work toward alternative, more flexible remote work arrangements, leading to a reallocation of labor in the economy. As the shock hits the economy, workers leave the jobs without the amenity (quits rise, and more so in the non-teleworkable sectors), which then become vacant (vacancies rise, and more so in the non-teleworkable sectors), and move to better jobs (EE rates increase). These vacant jobs are undesirable and hard to fill (aggregate match efficiency falls, and job filling rates decline more in the non-teleworkable sectors). Because the reallocation occurs mostly through job-to-job transitions, unemployment does not move much –but vacancies do– and the Beveridge curve moves vertically, as in the data. Finally, average wages in sectors with a larger share of teleworkable jobs fall more because these jobs offering the amenity become more attractive and command a negative compensating differential.²¹

2.4 Regression Analysis of Vacancies, Quits and Wages

We provide further empirical support for this mechanism using a regression framework, leveraging different data sources and show that: (i) quits predict the surge in vacancies, unlike earlier recoveries; (ii) job-to-job transitions between industries increased in the non-teleworkable sectors; (iii) the wage premium of teleworkable occupations declined significantly over this period.

Quits-induced vacancies. We find that post-pandemic quits rate is highly predictive of the vacancy rate at the industry-level suggesting that quits contributed to the vacancy stock by creating a need for replacement hiring. We estimate the following equation for three time periods that correspond to the cycles we compared in our earlier analysis:

$$\log y_{jt} = \alpha_0 + \alpha_q \log q_{jt} + \alpha_l \log l_{jt} + \alpha_o \log oth_{jt} + \beta_j + \delta_y + \epsilon_{jt} \quad (3)$$

²¹Reduced consumption of services during the lockdown, coupled with generous fiscal stimulus, directed consumer spending toward goods. Thus, a possible alternative explanation for the aggregate facts discussed in the previous section is that labor reallocation occurred from services into goods-producing sectors. In Figure C5 in the Appendix, we compare vacancies, employment, quits, and job filling rate in goods and services. We find that labor markets dynamics in these two sectors look extremely similar, and akin to the aggregate ones. The small sectoral differences observed are short lived, as they converge about 12 months after the onset of the shock, unlike the sizable and persistent divergences based on teleworkability which remained salient until 2022. Thus, the data do not support a demand shift from services to goods as a relevant source of labor reallocation. Rather, the driving force is a within-sector one.

	(1) 2020m1-2023m1	(2)	(3) 2008m1-2011m1	(4)	(5) 2001m1-2004m1	(6)
	<i>v</i>	<i>jfr</i>	<i>v</i>	<i>jfr</i>	<i>v</i>	<i>jfr</i>
Log Quits Rate	0.168*** (0.059)	-0.168** (0.073)	0.054 (0.061)	0.157** (0.062)	0.105 (0.072)	0.166** (0.065)
Log Layoff Rate	-0.106*** (0.018)	0.005 (0.026)	-0.162*** (0.045)	0.253*** (0.044)	-0.057 (0.040)	0.260*** (0.037)
Log Other Separations Rate	-0.019 (0.018)	0.033 (0.022)	-0.050** (0.023)	0.059** (0.024)	-0.076*** (0.024)	0.094*** (0.024)
Sector FE	Y	Y	Y	Y	Y	Y
Year FE	Y	Y	Y	Y	Y	Y
N	618	618	616	616	617	617
R ²	0.800	0.742	0.695	0.816	0.779	0.847

Table 1: Quits-induced vacancies that are harder to fill: Regression of vacancy rate and job filling rate.

Notes: JOLTS, 2001m1-2023m1, seasonally adjusted. *v* denotes vacancy rate (in logs), and *jfr* denotes job filling rate (in logs) defined as hires divided by vacancies. Robust standard errors in parenthesis. * $p < 0.10$, ** $p < 0.05$, *** $p < 0.01$.

where y_{jt} is the job openings rate or job filling rate in a NAICS 2-digit sector j in month t , q_{jt} is the quits rate which includes voluntary separations except retirements and transfers, l_{jt} is the layoffs and discharges rate which include involuntary separations initiated by the employer, oth_{jt} is other separations rate which includes separations due to retirement, death, disability, and transfers to other locations of the same firm, β_j includes sector fixed effects, and δ_y includes year fixed effects. Results are reported in Table 1.

Columns (1), (3), and (5) of Table 1 show that quits were positively correlated with the vacancy rate in the aftermath of the pandemic recession controlling for sector-fixed effects, but this was not true after the 2001 recession and the Great Recession when the correlation between vacancies and quits was insignificant. Since the JOLTS measures job openings that are open on the last business day of the reference month and quits during the entire reference month, this regression would capture positions that were left vacant by quits provided that the firm would want to replace the quitting worker. This notion of vacancies is consistent with the way we model the evolution of vacancies in Section 3.²²

²²We find that the relationship between quits, vacancies and job filling also holds in the cross-section. Industries with higher quits rates typically have higher vacancy rates and are able to fill their vacancies faster. This finding is reported in Appendix Table C1, columns (1), (3) and (5) which considers the sectoral correlation between vacancy and quits (and columns (2), (4) and (6) for job filling and quits). This cross-sectional correlation is even stronger if we control for layoffs and other separations. The correlation reflects

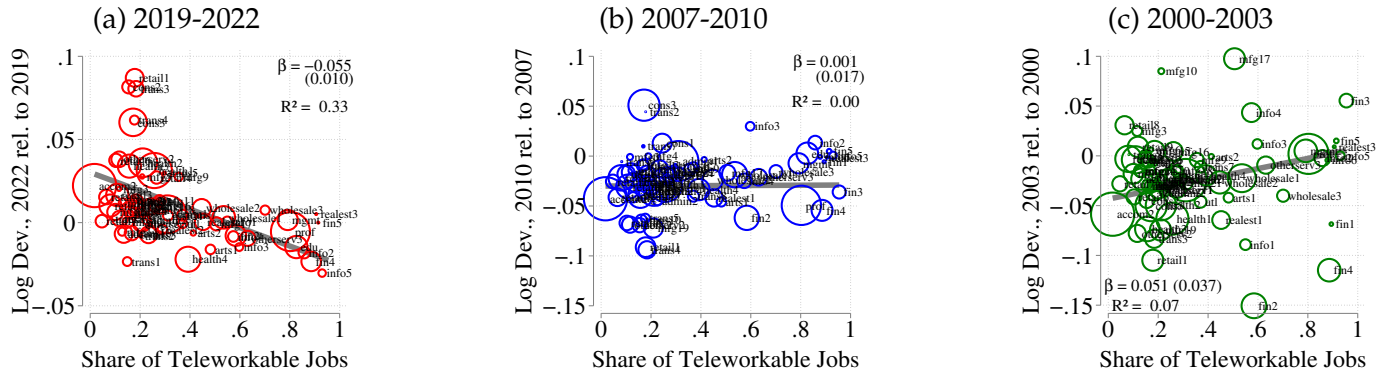


Figure 9: Labor reallocation between industries and teleworkability of industries: share of workers who switch industries during a job-to-job transition.

Notes: Each figure shows the share of workers who switch industries during a job-to-job transition plotted against the share of teleworkable jobs within the originating industry. Each circle represents a 3-digit NAICS industry and is labeled at the 2-digit level. Circle labels are defined in Table C2. Sizes of circles correspond to their employment share. Y-axis is in log deviation, and x-axis represents the share of teleworkable jobs in each 3-digit industry from Dingel and Neiman (2020). Panels a, b and c respectively exclude 2, 2 and 3 outlier industries accounting for 0.1% employment share. The gray line depicts the linear fit, and each panel indicates the coefficient, standard error (in parenthesis) and R-squared of the fitted line. *Source:* LEHD Origin-Destination Employment Statistics.

The mechanism we propose also implies that quit-induced vacancies were harder to fill due to the shift in workers' preferences toward remote work. Columns (2), (4), and (6) of Table 1 shows that higher quits rate were associated with lower job filling rates after the pandemic, while this correlation was positive in the earlier recoveries. These findings suggest that, during the post-pandemic recovery, sectors that saw both surging quits and high vacancy rates also experienced difficulties in filling those vacancies, resulting in markedly lower job filling rates.

Labor reallocation between sectors. The recently released job-to-job transition data by origin and destination industries for workers who changed jobs in the Longitudinal Employer Household Dynamics (LEHD) provide additional support for amenity-driven reallocation. For each of the 78 three-digit industries, we compute the share of job movers who also switch industries. Figure 9 plots the change in the share of between-industry job-to-job transitions against the share of teleworkable jobs within each originating industry from Dingel and Neiman (2020). Panel (a) shows that between 2019 and 2022, workers

the need for replacement hiring and is consistent across time periods.

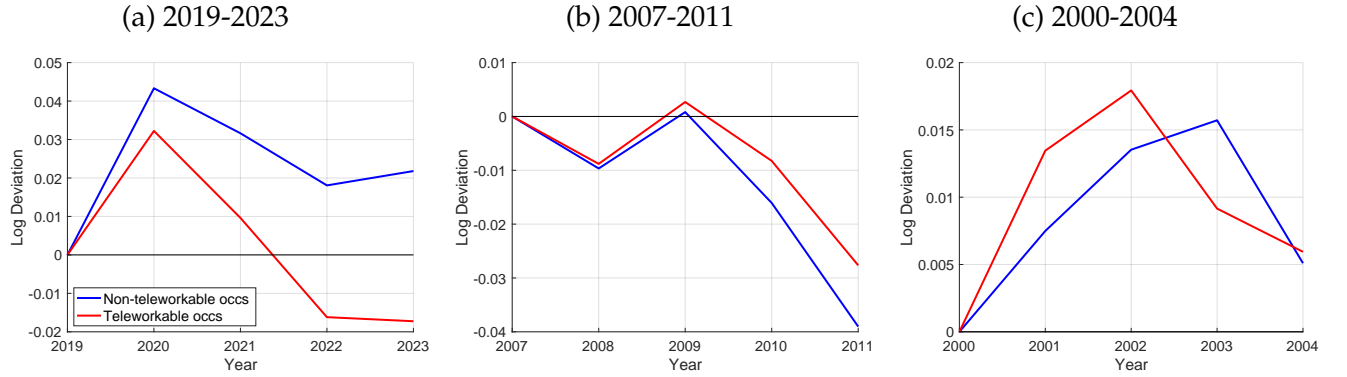


Figure 10: Residualized real wages per hour by teleworkability of occupations

Notes: Each figure depicts residualized average real hourly wages for teleworkable and non-teleworkable occupations. Wages are residualized for age, squared-age, education, race, and gender from Mincer regressions, and expressed as log deviations from the beginning of each sample year. Occupations are categorized as teleworkable or non-teleworkable using [Dingel and Neiman \(2020\)](#) classification. *Source:* Current Population Survey.

employed in less teleworkable industries were more likely to leave their industry when switching jobs, while those in more teleworkable industries tended to stay in their industry. In contrast, the relationship between teleworkability and between-industry job-to-job transitions was weaker –and even slightly positive– during the 2008 and 2001 recoveries (panels b and c). The gray line in each of the panels represents a linear fit of this relationship, with the substantially higher R-squared after the pandemic indicating greater predictive power of teleworkability in explaining inter-industry job-to-job transitions.

Relative wage dynamics Finally, we provide empirical evidence of a changing wage gap between teleworkable and non-teleworkable occupations consistent with the idea of a growing compensating differential for the ability to work from home. Specifically, we estimate the following Mincer-type regression:

$$\log w_{it} = X'_{it}\beta + \sum_y \delta_y \mathbb{I}\{Year_t = y\} + \sum_y \alpha_y \mathbb{I}\{Year_t = y\} * \mathbb{I}\{Telework_i = 1\} + \epsilon_{it}$$

where w_{it} is the real hourly wage of individual i in month t , X_{it} includes observables such as age, age-squared, education, gender and race, $\mathbb{I}\{Telework_i\}$ is an index function that takes value 1 if the individual is employed in a teleworkable occupation, y denotes

year, and ϵ_{it} is the error term. We estimate this regression specification for three sample periods: 2019-23, 2007-11, and 2000-04 using data from the Current Population Survey. Figure 10 plots coefficients δ_y and $\delta_y + \alpha_y$, respectively for workers in non-teleworkable and teleworkable occupations. Teleworkable wages used to grow similarly, if not faster than non-teleworkable ones in earlier recoveries. In contrast, a negative compensating differential clearly emerged in the post-pandemic period.²³

As already mentioned, these findings are consistent with those by [Barrero et al. \(2021\)](#) who report that around half of SWAA respondents are willing to accept significant pay cuts in exchange for 2 workdays a week of WFH. [Barrero et al. \(2022\)](#) find evidence that firms took advantage of this shift in worker attitudes in the April/May 2022 wave of the Survey of Business Uncertainty (SBU)²⁴. Specifically, they document that about four-in-ten firms reported that they expanded opportunities to work remotely in order to moderate wage-growth pressures in the past year. A similar number of executives reported that they expected to do so in the coming year.

We conclude by noting that this mechanism may have contributed to the so-called "unexpected wage compression" ([Autor et al., 2023](#)) in the post-pandemic period since non-teleworkable occupations, on average, pay less than teleworkable ones.

3 Model

Our empirical analysis identified some distinct features of labor market dynamics following the onset of the pandemic. Most notably, we have documented that the behavior of vacancies, quits, matching efficiency and prevalence of remote work all deviated from historical patterns. Informed by these observations, we set up a search and matching model equipped with the essential elements needed for a quantitative assessment.

3.1 Environment

The model is a version of [Lise and Robin \(2017\)](#) with three key extensions: (i) match specific productivity, (ii) a distribution of job amenities and heterogeneous valuation of amenities among workers, and (iii) Diamond entry and vacancies as a stock. The last two

²³The difference between red and blue lines in Figure 10 is significant at 5% level in panel (a), but not in the other two panels.

²⁴The Survey of Business Uncertainty a monthly survey administered to about 330 business executives. For details of the survey see: <https://www.atlantafed.org/research/surveys/business-uncertainty>.

features are crucial for the question we want to address since they allow us to connect to the data on quits and vacancies. In taking the model to the data, we will think of the job amenity mostly as the ability to perform job tasks remotely.

Time and shocks. The model is written in continuous time, as if the economy is following deterministic transitional dynamics determined by unforeseen ‘MIT shocks’. We allow for three sources of aggregate fluctuations: a shock to the preference for job amenities, a shock to productivity, and a labor supply shock to the value of unemployment.

Demographics and preferences. The economy is populated by a continuum of infinitely-lived workers of measure one who can be either employed or unemployed. Workers discount the future at rate r and have linear utility over consumption c_t which equals their income.

Unemployed workers receive a flow utility $b_t = Z_t^b b$, which we interpret as the combination of consumption (unemployment benefits) and the flow value of leisure. Z_t^b is an aggregate shifter of the flow value of unemployment.

Employed workers receive a flow wage payment w_t . Appendix D.1 describes the wage determination in detail. Employed individuals also obtain utility from a job amenity a . Let x denote the individual taste for (i.e., how much they value) the job amenity. The distribution of x across workers is exogenous, and denoted by $\ell(x)$. We assume that there exist two worker types with $x \in \{0, \bar{x}\}$, respectively. The variable Z_t^x is an aggregate shifter of the value of amenities. A worker of type x , employed in a job with amenity a at time t receives an additional utility flow equal to $Z_t^x xa$. Besides this dimension of heterogeneity, workers are equally productive ex-ante.

We can write the flow utility of a worker with amenity valuation x as

$$\mathcal{U}_t = \begin{cases} w_t + Z_t^x xa & \text{if employed in a job with amenity } a \text{ at wage } w_t \\ Z_t^b b & \text{if unemployed} \end{cases}$$

Production technology and income payments It takes one worker and one job to produce. A firm-worker pair produces an idiosyncratic output level $y \sim F$, where $F(y^*) := \Pr(y \leq y^*)$, which we assume to be a discretized log-normal distribution with mean 1 and dispersion parameter σ . This idiosyncratic output level remains constant for the duration of the match and is rescaled by aggregate productivity Z_t^y . Let $y_t = Z_t^y y$ denote the combination of individual-level and aggregate productivity,

Worker-firm matches are destroyed exogenously at rate δ . When an unexpected aggregate shock hits the economy, some matches may be endogenously dissolved.

Job types There are three types $n \in \{0, 1, 2\}$ of jobs in the economy. If matched, a job provides their worker with one of two distinct amenity flow values $a(n) \in \{\underline{a}, \bar{a}\}$ that depends on their type. We impose that $a(0) = a(1) = \underline{a}$ and $a(2) = \bar{a}$. That is, jobs of type $n = 0$ and $n = 1$ do not provide the amenity, whereas jobs of type $n = 2$ provide the amenity. Jobs of type $n = 1$ are different from jobs of type $n = 0$ in that they can, at Poisson intervals, choose to pay a randomly drawn cost and become a job of type $n = 2$. This process, which we will refer to as "upgrading", is described in detail at the end of this section.

This modeling choice captures the idea that whether a job is capable of providing the amenity (i.e. it is teleworkable) is a technological constraint of the economy: some jobs ($n = 0$) feature essential tasks that need to be performed on site, while others ($n \in \{1, 2\}$) do not, and are teleworkable. Among teleworkable jobs, some ($n = 2$) decide to provide the remote work amenity while the remainder of teleworkable jobs ($n = 1$) decide not to provide it. Following this interpretation, in what follows we will refer to jobs of type $n = 0$ as "non-teleworkable", jobs of type $n = 1$ as "passive teleworkable", and jobs of type $n = 2$ as "active teleworkable".

Meeting technology At time t , a measure $u_t(x)$ of workers of type x is unemployed, and a measure $e_t(x, y, n)$ of workers of type x is employed on matches of type (y, n) . The following consistency condition must hold for each type x .

$$u_t(x) + \sum_{y,n} e_t(x, y, n) = \ell(x) \quad (4)$$

The search intensity of the unemployed is normalized to 1. Let s denote the relative search effort of employed workers. The total number of job seekers s_t is then

$$s_t = \sum_x u_t(x) + s \sum_{x,y,n} e_t(x, y, n) = u_t + s e_t \quad (5)$$

Let $v_t(n)$ denote the vacancies of type n . The total number of vacancies is

$$v_t = \sum_n v_t(n) \quad (6)$$

Job seekers and vacancies meet at random. The total number of random meetings occurring at date t is given by the aggregate meeting technology

$$m_t = m(v_t, s_t), \quad (7)$$

where m is a CRS meeting function. Let $p_t = m_t/s_t$ be the meeting rate for the unemployed, $p_t s$ the one for the employed, and $q_t = m_t/v_t$ the one for vacancies.

The draw of idiosyncratic match productivity y occurs right after a meeting is formed. Not all meetings transform into productive matches. In Section 3.2, we describe the match formation decision.

Job creation. There is free entry of firms in the economy, and a sufficiently large supply of potential entrants that the ex-ante value of entry never exceeds zero at every t . To become an incumbent, a potential entrant pays an entry cost κ . Once the vacant job is created, but before it starts searching for a worker, it randomly draws its job type. We assume that newly created jobs take type $n = 1$ with probability ζ and type $n = 0$ with probability $1 - \zeta$. As a result, among jobs that newly enter the economy, there is always a share ζ of jobs endowed with the technology to provide the amenity (teleworkable) and a share $1 - \zeta$ without it (non-teleworkable). The ex-ante value of entry is thus given by

$$\zeta \Omega_t(1) + (1 - \zeta) \Omega_t(0) = \kappa \quad (8)$$

We let $i_t \geq 0$ denote the number of new jobs which sets the expected value of entry to zero.

Vacancies as a stock and vacancy chains. Because the entry cost is sunk for an incumbent, the value of a vacancy is weakly positive. As a result, entrant vacancies that do not immediately get filled stick around and contribute to the pool of idle jobs ready to hire.

In this model, vacancies are not a jump variable, as in standard search-matching models. At any time t , the stock of vacancies is a backward looking variable that depends on the past stock, the inflow into the stock and the outflow from the stock. The outflow has two components. First, vacancies exit exogenously at rate δ_v . Second, some vacancies get filled by job seekers. Likewise, the inflow has two components. First, the newly created job opportunities i_t . Second, the jobs vacated by quits. We assume that upon a quit or an exogenous separation (occurring at rate δ), the vacant job enters a ‘dormant state’ in

which the firm is not actively recruiting. Dormant vacancies re-enter the pool of actively searching vacancies stochastically at Poisson rate μ .²⁵

Note that the model features ‘vacancy chains’ and ‘replacement hires’, i.e. situations where a worker quits their job, the job becomes vacant, and a new employed worker is hired on the same job to replace the previous employee, leaving another vacant job behind them.

Upgrading Filled and vacant jobs of type $n = 1$ encounter stochastic opportunities to become jobs of type $n = 2$ (i.e. to “activate” the amenity) with exogenous Poisson rate π and $\vartheta\pi$, respectively. When such an upgrading opportunity arises, the job draws a cost c from a uniform distribution $G(c) = \frac{\lambda}{\pi}c$ with $c \in [0, \frac{\pi}{\lambda}]$. Vacant jobs choose whether to pay the cost of upgrading c and transition into state $n = 2$ or to pass up the opportunity and keep searching as type $n = 1$. For filled jobs, we assume that workers and firms contractually commit to making an upgrading decision that maximizes their joint gross surplus and that the upgrading cost is borne by the firm. As shown in Appendix D.2, the choice of π turns out to be irrelevant provided that π is sufficiently large, which we assume henceforth.

3.2 Surplus Determination and Rent Splitting

Surplus definition. Let the gross surplus of a match of type (x, y, n) at date t be

$$S_t(x, y, n) = J_t(w_t, x, y, n) + W_t(w_t, x, y, n) - U_t(x) \quad (9)$$

where J is the value of a match for the firm and W for the worker, and U is the value of unemployment. Note that this ‘gross’ surplus definition does not include the outside option for the firm²⁶.

²⁵We include this dormant state primarily for numerical stability. Without it, separations that occur in a particular state immediately raise the number of vacancies, which discontinuously lowers the value of a vacancy for new entrants. This introduces numerical instability in the solution algorithm, which relies on a fixed point of this value. The dormant state ensures that vacancy inflows from separations are spread out over time, which in practice helps with the convergence of the solution algorithm. Qualitatively and quantitatively, our results are robust to even large values of μ .

²⁶Depending on whether a job is filled or vacant, the outside option of the firm can be either the value of an active or a dormant vacancy. For this reason, it is more convenient to define the ‘gross’ surplus, which does not include this outside option.

Wage setting. We assume the sequential auction contract renegotiation protocol of [Postel-Vinay and Robin \(2002\)](#). Wages can only be renegotiated under *mutual consent*, i.e. when either side has a credible threat. A *credible threat* occurs when one of the parties is better off taking their outside option than staying in the match (i.e. one of the two participation constraints is violated). Upon renegotiation, or upon meeting between a vacancy and an unemployed worker, we assume that the firm makes a take-or-leave offer to the worker. The events that can trigger renegotiation occur when a suitable outside offer is made to the worker by another firm, or when an aggregate shock changes the value of either party sufficiently. We also assume that wages do not change upon an upgrade unless the upgrading decision induces a credible threat for dissolution by either party. The details of our wage setting protocol are collected in Appendix [D.1](#).

Surplus dynamics. An implication of our wage setting protocol is that the surplus becomes independent of the wage (see [Lise and Robin, 2017](#), for details). In Appendix [D.4](#), we show that the surplus of an ongoing match can be written as

$$(r + \delta)S_t(x, y, n) = Z_t^y y + Z_t^x x a(n) - Z_t^b b + \mathbb{I}_{\{n=1\}} \frac{\lambda}{2} (S(x, y, 2) - S(x, y, 1))^2 + \delta \tilde{\Omega}_t(n) + \partial_t S_t(x, y, n) \quad (10)$$

with the boundary condition $S_t(x, y, n) \geq \tilde{\Omega}_t(n)$, where $\tilde{\Omega}_t(n)$ denotes the value of a dormant vacancy of type n . The term multiplying the indicator function is the expected gain from upgrading under our distributional assumption.

Bilateral efficiency. A key property of this economy, stemming from the wage protocol described above, is bilateral (or joint) efficiency which implies that all decisions within a match –hiring, separation and upgrading (the latter by assumption)– are obtained by comparing surpluses associated with the alternative options. As a result, wages are not allocative and only split the surplus of a match. Thus, all allocations can be calculated without knowledge of the wages, which lends great tractability to the problem.

Solution method Equation (10), which governs the surplus dynamics, reveals that the model is not block-recursive as in [Lise and Robin \(2017\)](#). The reason is that the firm outside option $\tilde{\Omega}_t$ is not zero, and it depends on equilibrium distributions. Solving for an equilibrium therefore requires an additional outer loop over Ω_t , but it remains perfectly

Parameter		Value	Target to match	Target value
Discount rate	r	0.05/12	<i>External</i>	
Elasticity of meeting function	α	0.50	<i>External</i>	
Re-entry rate dormant vacancies	μ	1.0	<i>External</i>	
Share of workers with $x = \bar{x}$	$\ell(\bar{x})$	0.50	<i>Barrero, Bloom & Davis (2021)</i>	
Entry cost	κ	2.02	Meeting rate of unemployed	1.5
Opportunity cost of work	b	1.01	UE rate	0.30
Search effort of employed	s	0.78	EE rate / UE rate	0.07
Separation rate	δ	0.015	EU rate	0.015
Vacancy destruction rate	δ_v	0.33	Share of replacement hires	0.50
Productivity dispersion	SD(log y)	0.042	Short run response of unemp. to Z^y	
Amenity scale	\underline{a}, \bar{a}	-0.11, 0.89	Long run response of output to Z^x	0
Preference weight on amenity	\bar{x}	0.048	Compensating differential	0.025
Prob. of TW job creation	ζ	0.33	Share of teleworkable employment	0.37
Upgrading cost parameter	λ	$5.0 \cdot 10^{-4}$	Active TW employment share	0.10
Rel. vacancy upgrading rate	ϑ	63.2	Active TW new vacancy share	0.05

Table 2: Parameters and corresponding targets. The model period is one month.

feasible and quite fast.

This concludes the description of the model. Since some equations are lengthy but all derivations are fairly standard, we relegate the characterization of the value functions and laws of motion to Appendix D, where we also formally define a perfect foresight equilibrium of the model, and explain in detail how to compute it numerically.

4 Parameterization

We parameterize the model in two blocks. Parameters in the first block are set externally and based on existing literature. Parameters in the second block are set internally to match moments from the data. Table 2 summarizes the parameter values and the targeted moments. The model period is one month.

The first parameter block consists of the meeting function elasticity α , the discount rate r , and the share of high x workers $\ell(\bar{x})$. We set the elasticity of the meeting function α to 0.5 and the discount rate r to 5% annually. Next, we impose a re-entry rate μ of dormant vacancies equal to 1.0. Lastly, we set the share of high x workers to 0.5, consistent with evidence from [Barrero, Bloom, and Davis \(2021\)](#) who find that about half of workers in the population would be willing to accept positive wage cuts in exchange for the ability to work from home.

We divide parameters of the second block into those which more directly impact equilibrium labor market flows, and those related to the prevalence and value of the amenity, i.e. teleworkability.

We set κ and b to jointly generate a monthly encounter rate of 1.5 (Faberman et al., 2022) and a monthly UE rate of 0.3 (a long-run average in the CPS). We choose the relative search intensity of the employed, s , to match an EE/UE ratio equal to 0.07. The separation rate δ is set to match an EU rate of 0.015, consistent with a long-run average from CPS data. We set the vacancy destruction rate δ_v in order to match a share of vacated vacancies (i.e. vacancies created through quits) of 0.5, a number consistent with evidence presented in Acharya and Wee (2020) and Qiu (2024). The match-specific productivity dispersion σ governs the sensitivity of our model to aggregate productivity shocks. We choose it in order to generate an initial response of the unemployment rate of 0.5 log points to a -7% productivity shock, consistent with the initial dynamics of the COVID recession in which output per worker initially decreased by 7% and unemployment rose by about 0.5 log points.

The distance between \underline{a} and \bar{a} is normalized to one and we choose the two values in order to set the response of output to a moderate sized x shock (0.025) to zero in the long-run. Put differently, we take the view that the shift in work arrangements is roughly neutral on productivity²⁷. The preference weight on amenity \bar{x} is chosen to generate a small compensating differential (defined as $\frac{1}{2} \frac{\bar{x}(\bar{a}-\underline{a})}{w}$) of 0.025 in the initial steady state. Next, ζ , the share of teleworkable jobs created is set to match the overall share of teleworkable employment in the economy, 37% as found in Dingel and Neiman (2020). The upgrading cost parameter λ is set to target the share of employment working from home in the initial pre-pandemic steady state (Barrero et al., 2021). Finally, we set the relative upgrading rate of vacancies ϑ to match the initial share of newly created vacancies (i.e. vacated or newly entered and upgraded) that are active teleworkable. The empirical counterpart of this theoretical moment is the pre-pandemic share of new job vacancies explicitly advertising the ability to WFH (Hansen et al., 2023).

²⁷Evidence on the effect of remote work on idiosyncratic productivity has been mixed, with some studies pointing to positive impacts (Bloom et al., 2015; Cullen et al., 2025), and others to negative ones (Emanuel and Harrington, 2024)

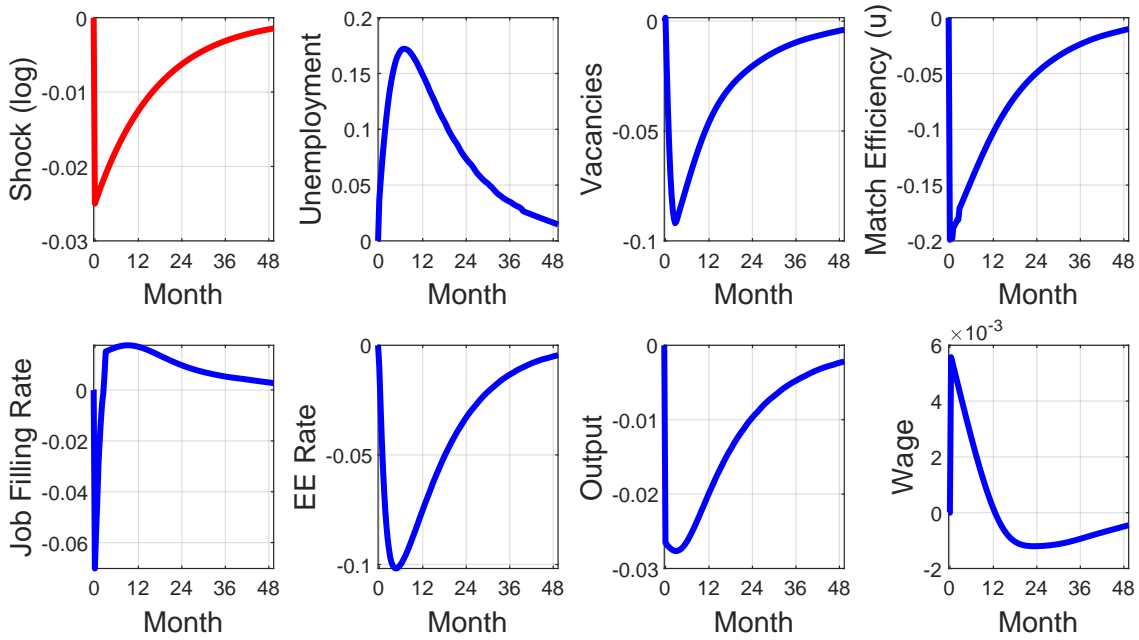


Figure 11: Impulse response functions to a productivity (y) shock. The path for the shock is plotted in the top-left panel in red. Log deviations from initial steady state.

5 Impulse Response Functions

We now illustrate how the model responds to an unanticipated innovation in each of our three aggregate shocks Z^s , $s \in \{y, b, x\}$. An innovation of size ε_0^s that hits at time $t = 0$ induces a path for the shock given by

$$Z_t^s = e^{-\rho_s t} \varepsilon_0^s, \quad \text{for } t \geq 0 \quad (11)$$

We assume that the b shock reverts very quickly, with $\rho_b = 0.23$, implying that it takes about two years to fade out completely. This fast mean reversion reflects the observation that UI benefits extensions during recessions are, typically, short-lived.²⁸ For the productivity shock, we set $\rho_z = 0.057$, corresponding to a half-life of one year, and about 5 years until the shock dissipates entirely. We assume that innovations to the amenity shock are permanent ($\rho_x = 0$), i.e. they generate long-lasting shifts in preferences.

Figure 11 displays the impulse response of some key aggregate variables to a negative

²⁸With the exception of the Great Recession, in all the downturns since 1970—including the pandemic one—UI extensions lasted around two years.

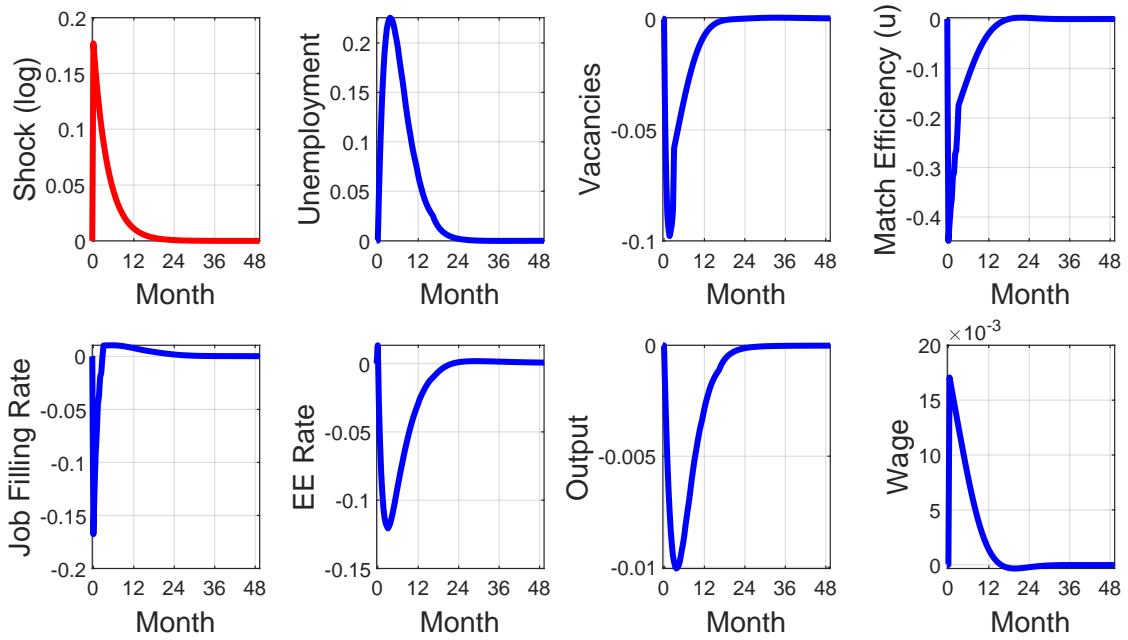


Figure 12: Impulse response functions to the opportunity cost of work (*b*) shock. The path for the shock is plotted in the top-left panel in red. Log deviations from initial steady state.

productivity shock. The resulting dynamics are much like those that a standard frictional model of the labor market would deliver. As productivity falls, the incentive to post vacancies decreases and vacancies rapidly decline as entry dries up. Falling vacancies reduce the job finding rate, which results in an increase of the unemployment rate. Because aggregate productivity is lower, it becomes less likely that a worker-firm pair draws an idiosyncratic productivity high enough to make the match viable, and thus match efficiency decreases. Since match efficiency is a jump variable but vacancies are sluggish, the job filling rate falls on impact. Then, the drop in vacancies more than offsets the decline in match efficiency and the reduced congestion leads the job filling rate to rise above steady state persistently. The EE rate falls because the stock of vacancies decreases (i.e., jobseekers make fewer contacts) and match efficiency falls (i.e., fewer contacts become matches). Output falls as a direct consequence of lower productivity. The wage dynamics are non-trivial: average wages increase in the short-run because of a strong initial selection effect: surviving matches are now more productive. However, over time, the lower productivity pulls wages below trend persistently.

The impulse responses to a negative labor supply shock (a rise in the opportunity cost of work *b*) depicted in Figure 12, deliver similar dynamics. This is not surprising: since

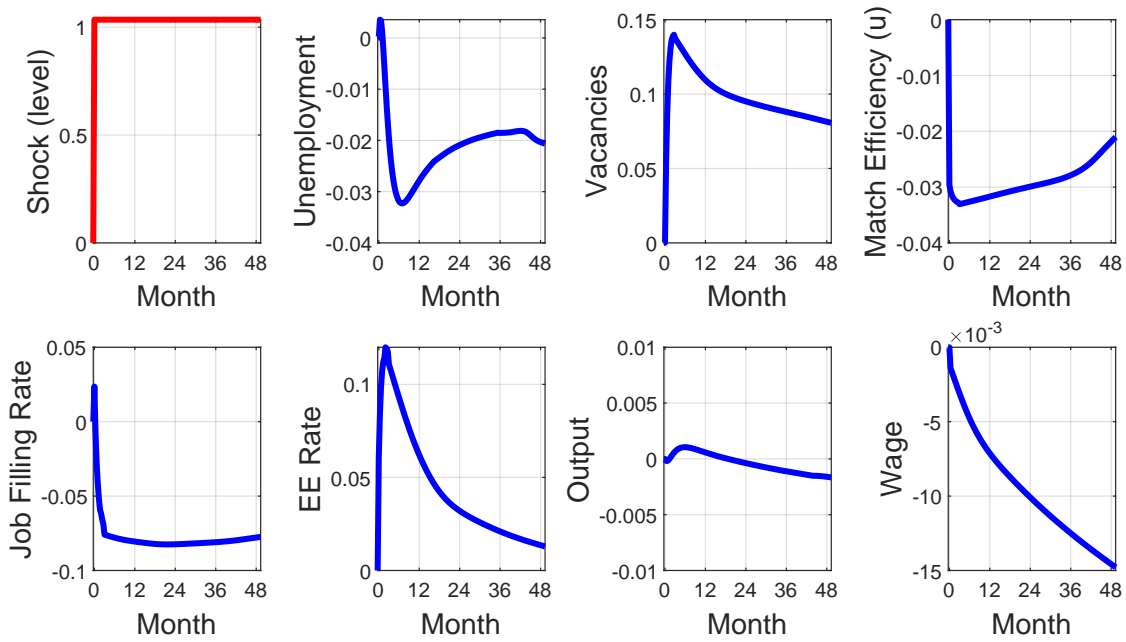


Figure 13: Impulse response functions to an amenity valuation (x) shock. The path for the shock is plotted in the top-left panel in red. Log deviations from initial steady state.

allocations in our model depend solely on the surplus, and y and b enter the surplus additively, there is an equivalence between shocks to b and shocks to y of the opposite sign.²⁹ Wages, however, respond differently to productivity and labor supply shocks. As illustrated in the last panel of Figure 12, a rise in b strengthens workers' outside option and leads to a sustained rise in average wages. As opposed to negative productivity shocks, wages never fall below steady state.

Labor market dynamics following a shock to the household valuation of the amenity x are displayed in Figure 13. For workers with $x = \bar{x}$, the shock increases the value of being matched to a high amenity job (especially active ones with $n = 2$), and decreases the value of working on a low amenity job ($n = 0$). Thus, high- x workers wait for an opportunity to quit into another job in order to leave their low amenity employer behind. These workers vacate their jobs, and the affected firms start searching for a replacement. The surge in low-amenity vacancies drives the increase in the overall stock of vacancies. However, these idle positions are hard to fill in the post-shock environment because they are less likely to be accepted by high- x workers which make up for half of the population. As

²⁹The equivalence is not an isomorphism since Z_i^y enters multiplicatively and therefore affects the dispersion of y in the population.

a result of this adverse compositional change in the vacancy pool, match efficiency falls. The combination of higher vacancies and lower match efficiency depresses the job filling rate. Slowly, as low amenity vacancies get filled mostly by low- x workers and disappear from the vacancy pool, the balance shifts back to an environment with more vacancies featuring an active amenity (i.e., upgrading from $n = 1$ to $n = 2$ occurs more frequently) whose value has increased. As a result, match efficiency recovers but the large number of vacancies keeps the job filling rate persistently low. The increased propensity of high- x workers in low- a jobs to reallocate to a new job pushes up the EE-rate. Notably, wages fall substantially as high- x workers are willing to accept matches with lower productivity on high-amenity jobs. This is also the reason why the shock has a very small, but negative, effect on aggregate output.

Finally, note that the rise in vacancies is much larger than the drop in unemployment, which prompts a vertical movement of the economy in the Beveridge space. This is a critical difference relative to the IRFs with respect to the y and b shocks which trigger much flatter dynamics in the Beveridge space, as clear from the two central panels of Figures 11 and 12.

5.1 Estimation of Aggregate Shocks

The model's impulse response functions (IRFs) imply a unique relationship between a sequence $\{Z_t^s\}_{t=0}^T$, $s \in \{y, b, x\}$, of shock realizations (e.g., a time path for the productivity shock) and sequence $\{d_t^k\}_{t=0}^T$, $k = 1, \dots, K$, of a model's aggregate variable (e.g., a time path for vacancies). Our aim is to leverage these IRFs to estimate the realized path of the three aggregate shocks from observed time series data for the US labor market. To obtain the series of realized shocks that, through the lens of the model, is most consistent with the data, we minimize the distance between a number of model-implied time series and their empirical counterparts.

Consistently with the way we compute IRFs, we assume that stochastic innovations are unanticipated (i.e., MIT shocks) and trigger a perfectly foreseen transition for the shocks given by (11), and for the aggregate variables d^k given by the model's deterministic equilibrium dynamics. Thus, when we simulate the model's equilibrium time series induced by a sequence of shocks, effectively agents are continuously surprised by each new innovation (as in Boppart et al., 2018).

Another key assumption that allows us to make progress is that the response of the equilibrium system can be effectively summarized as a sum of past (possibly nonlinear)

functions of the innovations. Formally, for any history of innovations $\{\varepsilon_t^s\}_{t=0}^T$ and some model series $\{d_t^k\}_{t=0}^T$, we assume that each realization d_t^k can be represented as

$$d_t^k = \sum_{s \in \{y, b, x\}} \sum_{j=0}^t h_{s,j}^k(\varepsilon_{t-j}^s) \quad (12)$$

where the function $h_{s,j}^k(\varepsilon_{t-j}^s)$ is implied by the model. This function describes the response of the variable k at date t to an innovation to s of size ε^s which occurred j periods ago. This formulation allows for responses to shocks that are *size- and sign-dependent*.³⁰ Allowing for such size- and sign-dependence is crucial because many impulse responses that we compute turn out to be highly non-linear in the size of the shock and are asymmetric.

To obtain an approximation of $h_{s,j}^k$, we first compute the impulse responses to each aggregate innovation ε^s , $s \in \{y, b, x\}$ starting from the initial steady state, at different horizons and for different shock magnitudes, both positive and negative. This set of impulse responses allows us to compute $h_{s,j}^k$ for any horizon j evaluated at this set of shock values. We obtain $h_{s,j}^k$ for any shock size by interpolating the function. Effectively, in simulating the model using IRFs we are assuming that agents are continuously surprised by each innovation

Finally, to estimate $\{\varepsilon_t^s\}_{t=0}^T$, we first compute the relevant empirical counterparts \hat{d}_t^k from the data. Then, we numerically solve

$$\{\varepsilon_t^s\}_{s,t} = \arg \min \underbrace{\sum_{k=1}^K \sum_{t=0}^T \omega_k \left(\hat{d}_t^k - \sum_{s \in \{y, b, x\}} \sum_{j=0}^t h_{s,j}^k(\varepsilon_{t-j}^s) \right)^2}_{\text{Series fitting}} + \underbrace{\vartheta \sum_{s,t} (\Delta \varepsilon_t^s)^2}_{\text{Smoothing}} \quad (13)$$

which yields the underlying shock series $\{\varepsilon_t^s\}_{t=0}^T$, with $s \in \{y, b, x\}$.

Two objects of this minimand are worthy of further discussion. First, there is a vector of series-specific weights ω_k .³¹ Second, we include a smoothing term in our objective function, with parameter ϑ . The purpose of this term is to prevent estimates that imply

³⁰For example, a large shock might trigger a different response than two shocks that are half the size and the same sign. Likewise, a positive and a negative shock of the same size might trigger asymmetric responses.

³¹For most variables, we choose a weight ω_k to equal the inverse variance of the respective data series. This ensures that variables with large fluctuations around the steady state do not dominate the fitting procedure. As we are particularly focused on unemployment and vacancies, and on their joint dynamics, the Beveridge curve, we choose a higher weight (factor 10) for unemployment and vacancies.

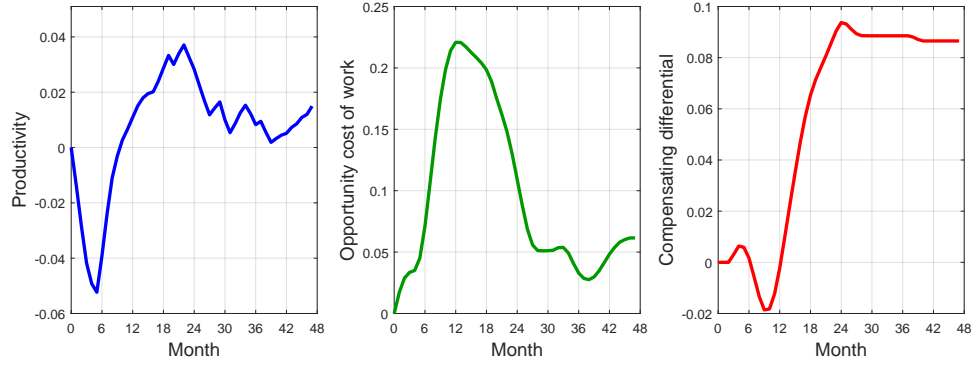


Figure 14: Estimated path of productivity Z^y (log-deviations), opportunity cost of work Z^b amenity shock Z^x . Log-deviations from initial steady state.

alternating and large positive and negative shocks in quick succession.³²

We choose eight time series (i.e., $K = 8$) for this minimization exercise: the unemployment rate, aggregate vacancies, match efficiency of the unemployed, the job finding rate, the job filling rate, the EE rate, aggregate output, and average wages.³³ The sample period we use in the estimation is 2020:1-2023:12 (i.e., $T = 48$). Because we use many more series than shocks, one should not expect a perfect fit of the data.

In closing, we note that our estimation strategy builds on the filtering approach proposed by McKay and Wieland (2021) who show how to implement the Kalman filter to recover the shocks that generated observed aggregate time series data using only impulse response functions, and not relying on a state space representation of the model. We generalize their approach to allow for non-linearities and sign-asymmetries, building on Reiter (2018).

6 Results

We now explore whether, and how, our model can quantitatively explain the peculiar dynamics of the post-pandemic labor market we described in Section 2 in three steps: (i) we report the estimated shocks; (ii) we present the fit of the model, and decompose the responses to isolate the contribution of the three aggregate shocks; (iii) we present additional results that shed light on the forces at work in the model. We conclude by ex-

³²In practice, we find that $\vartheta = 2000$ produces a good balance of smoothness and goodness-of-fit.

³³The UE rate can be obtained from unemployment, vacancies and match efficiency for the unemployed, all targeted time series as well.

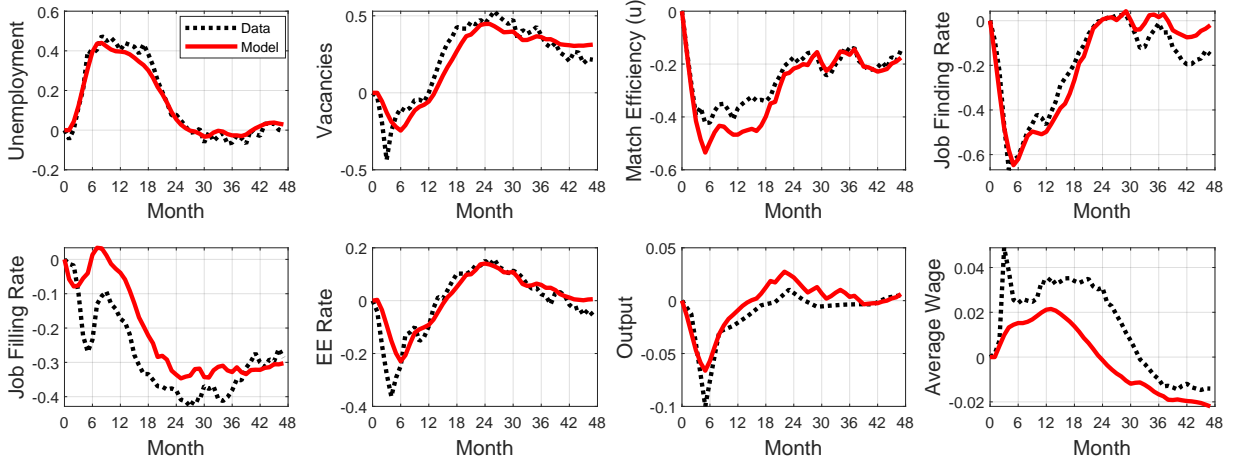


Figure 15: Model-simulation fit of the data. Data in black dashed line and model in solid red line. Log-deviations from initial steady state.

ploring the alternative view that the rise in work-from-home was not driven by a change in workers' attitudes under stable technology, but rather by a technological shift under stable preferences.

6.1 Estimated Shocks

Figure 14 illustrates the estimated paths for the three shocks. The productivity shock Z^y (left panel) displays a sharp fall of around 5% over the period that roughly corresponds to the time of lockdowns and restrictions of social and economic activity, followed by a quick but robust rebound which peaks at 4% above steady state, and a gradual return toward trend. The strong rebound in productivity also captures “pent-up spending” forces which are absent from our framework because we refrained from explicitly modeling aggregate demand channels.

The labor supply shock Z^b (middle panel) indicates that the opportunity cost of working increased by over 20 percent over the first year and a half following the shock, and then subsumed thereafter. This shock is a catch-all for three factors which played a major role during this recovery, all of which are expected to reduced the relative value of working: (i) the deteriorating health conditions of part of the workforce, especially early in the sample period; (ii) the vast expansion in size and eligibility of UI benefits; (iii) the generous fiscal transfers to low-income households.

Our novel shock to the value of the job amenity Z^x is plotted in the right panel of

Figure 14. This path displays a gradual build-up which reaches a peak around two years after the onset of the pandemic, after which the shock levels off. We have expressed the size of the shock as the compensating wage differential that, on average, a worker would be willing to pay in order to obtain the amenity in their current match. Quantitatively, the model tell us that the average value of job amenities increased from a small initial compensating wage differential of 2.5% to 11%. Results from a representative survey fielded after the pandemic by [Barrero et al. \(2021\)](#) suggest that respondents are willing to accept pay cuts around 8%, on average, for the option to work from home two or three days per week. More recently, a survey of workers in the tech sectors estimates an average willingness to forego 25% of total compensation in order to have a –partly or fully– remote instead of an in-person position ([Cullen et al., 2025](#)). Our estimated path for Z^x is broadly in accordance with these data points.

6.2 Model Fit and Shock Decomposition

Figure 15 plots the model’s fit of the time series we use in the estimation against the data. Overall, the fit is quite good, in spite of the model being overidentified.

Which aggregate shock is responsible for the dynamics of these different dimensions of the US labor market? Figure 16 plots model counterfactuals where we add one shock at the time.³⁴

The productivity shock (blue line in Figure 16) plays a dominant role in explaining the dynamics of the economy over the first 6 months, in particular the quick rise in the unemployment rate, as well as the dip of vacancies, match efficiency, job finding rate, EE rate, and output. However, the sharp rebound in productivity which follows the initial short-lived, but deep, recession generates counterfactual dynamics for many model series: an excessive drop in unemployment and average wage (due to negative selection into employment), and an exaggerated increase in match efficiency, job finding rate, job filling rate, and output.

The negative labor supply shock (a rise in b) more than offsets the rebound in productivity during the recovery. As a result, the sum of these two shocks (green line in Figure 16) accounts well for the rise in unemployment, as well as the drop in match efficiency and UE rate observed over this period. Also the fit for output is improved, since a larger b reduces employment. At the same time, though, this shock is so powerful that it substantially depresses vacancy creation. As a consequence, the model is still far from matching

³⁴The order does not matter because of the additive separability assumption discussed in Section 5.

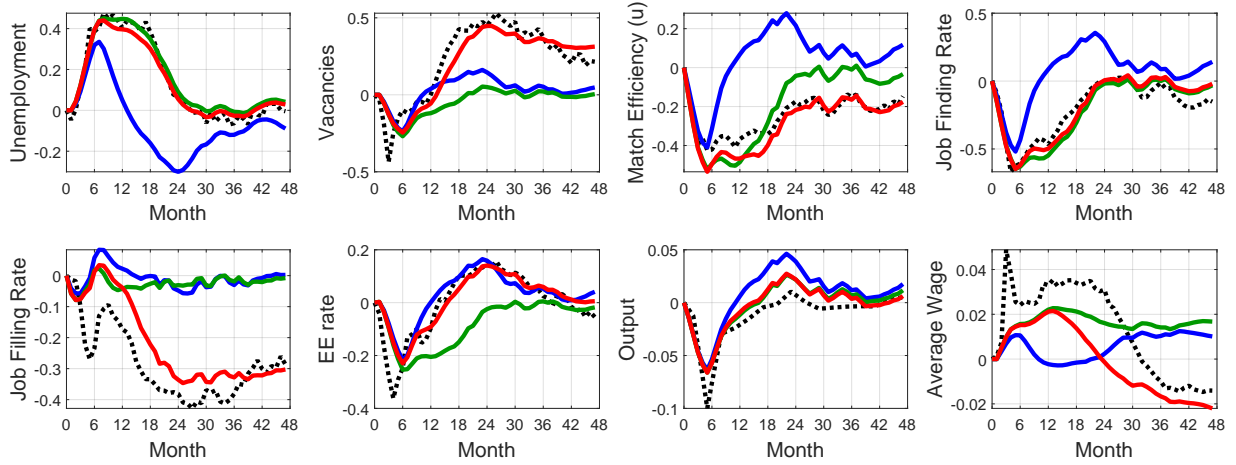


Figure 16: Decomposition of model's fit of the data (black dotted line) into productivity shock (blue), productivity + labor supply shocks (green) and productivity + labor supply + amenity shocks (red). The red line is also the model's fit to the data. Log-deviations from initial steady state.

the fall in the job filling rate, and implies a counterfactual decline in the EE rate. Notably, the labor supply shock can explain much of the rise in real wages in the first two years after the pandemic, and part of its decline.

The rise in the value of job amenities \bar{x} plays a crucial role in explaining the data because it accounts for virtually the entirety of the rise in vacancies and the fall in the job filling rate. This force also sets in motion a labor reallocation process that leads to a persistent rise in job-to-job transitions. Another important feature of the amenity shock is that it contributes to the protracted reduction in average real wages observed in the data, especially in the last 12 months of our sample period. We conclude by noting that [Barrero et al. \(2022\)](#) estimate that the shift to remote work moderated aggregate wage growth cumulatively by around 2 pct in the two-year period centered around April 2022, a magnitude similar to the one implied by our model.

6.2.1 Beveridge curve

Figure 15 showed that the model closely matches both unemployment and vacancies. Figure 17 plots the Beveridge curve implied by the model and its decomposition into the three shocks. The model is able to generate the wide Beveridge loop observed in the data. In particular, the plot displays the vertical section of the Beveridge curve where vacancies rise without virtually any change in unemployment.

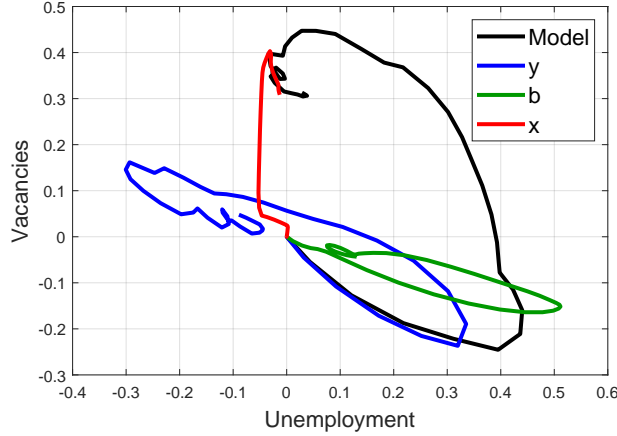


Figure 17: Model's Beveridge curve (dotted black line). Dynamics induced by shocks to productivity (blue), opportunity cost of work (green), and amenity value (red). Log-deviations from initial steady state.

From the decomposition, it appears that the productivity and labor supply shocks alone would have led to a narrow and flatter loop, as in all previous recessions (recall Figure 1). Instead, the amenity shock induces a process of quits-induced vacancies and persistent worker reallocation, largely through EE transitions which leave unemployment unaffected, resulting in a steep movement of the curve.

6.2.2 Cross-sectoral implications

We now confront the cross-sectoral evidence presented in Section 2, where we showed that in the first 24 months of our sample period, the rise in vacancies, EE transitions and wages, and the fall in the job filling rate are much more pronounced in sectors with a low share of teleworkable jobs.

We did not explicitly model different sectors of the economy. However, within our model one can think of sectors with different shares of teleworkable jobs as random collections of jobs with different shares of type $n > 0$. Figure 18 illustrates the two extreme cases of 'artificial' sectors with share equal to zero and one. The plot shows that the model is consistent with the empirical patterns: high- x workers quit the low- a jobs for better jobs (higher EE rate in the low-amenity sector); these quits create vacant positions (stronger rise in vacancies in the low-amenity sector); these vacant positions are undesirable for a sizable part of the workforce (larger drop in the job filling rate in the low-amenity sector); because they are undesirable, these jobs command a compensating wage differential (higher relative wage growth in the low-amenity sector).

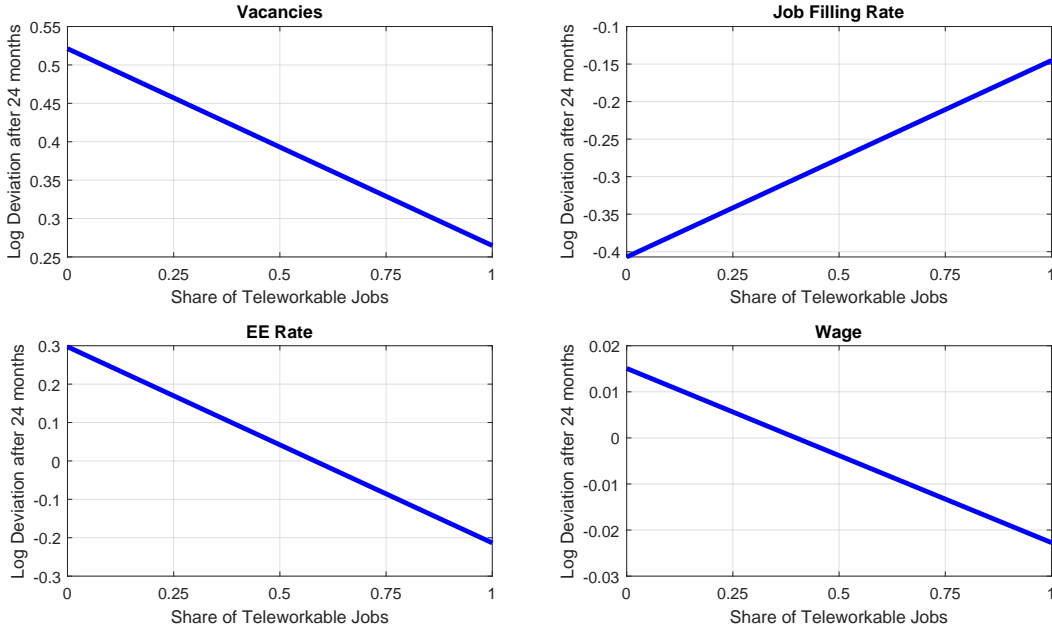


Figure 18: Model's counterpart of the cross-sectoral evidence of Figure 8.

6.3 Inspecting the Mechanism

In this section, we inspect in more depth the three key channels of the model transmission mechanism: (i) the labor reallocation induced by the amenity shock; (ii) the dynamics of the compensating wage differentials which rationalizes this reallocation; (iii) the associated change in the composition of the vacancy pool.

Labor reallocation. Figure 19 shows that the rise in the value of the job amenity induces a wave of labor reallocation that corrects the initial misallocation of worker types on job types emerging after the shock. High- x workers move toward high amenity jobs (middle panel), whereas low- x workers are willing to take the low amenity ones which now pay a larger wage premium to compensate for their lost appeal (left-panel). There is also a shift of workers who value the amenity from passive teleworkable to active teleworkable jobs (right panel).

Relative wage dynamics. Figure 20 illustrates the dynamics of wages for different worker and job types. High- x individuals are now willing to accept a negative compensating wage differential in order to work on an active teleworkable job (left panel). As a result, after the initial increase in wages across the board due to the rise in b , their own wages fall significantly. Low- x workers, in contrast, do not observe this decrease. These worker-

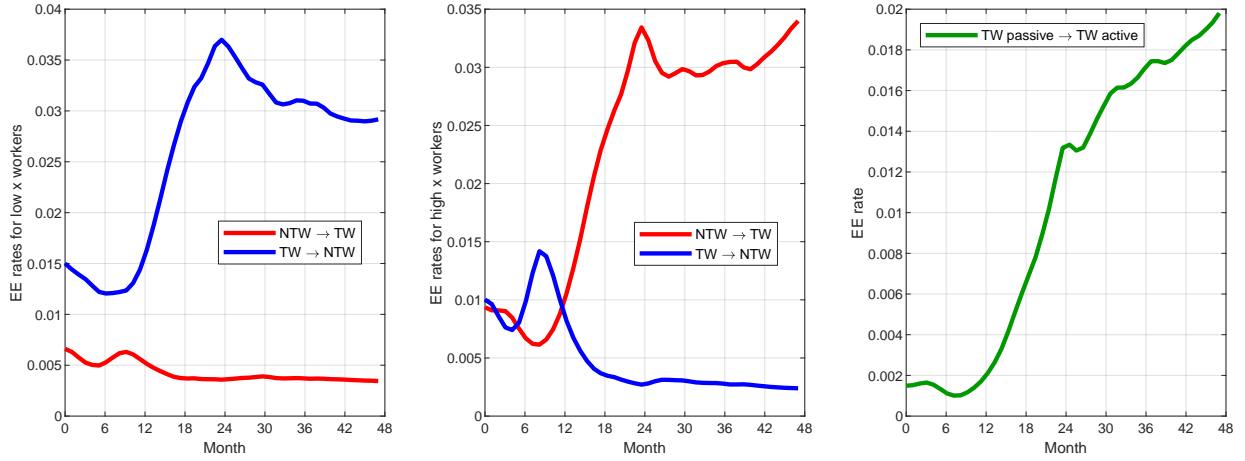


Figure 19: EE rates for low- x workers (left panel) and high- x workers (middle panel) between non-teleworkable ($n = 0$) and teleworkable ($n \in \{1, 2\}$) jobs. The right panel plots EE rates from passive teleworkable ($n = 1$) to active teleworkable ($n = 2$) jobs.

level wage dynamics are reflected also on the firm side (right panel) across the different types of jobs. Note that part of the decline in wages on active teleworkable jobs is due to the lower reservation productivity needed to create matches with high- x workers.³⁵

Composition of the vacancy stock. Vacancy dynamics are the mirror image of the labor reallocation described in Figure 19. The left panel of Figure 21 illustrates the dynamics of the stock of vacancies across the three job types $n \in \{0, 1, 2\}$. The change in composition of the vacancy stock takes place because teleworkable jobs become coveted by workers, while non-teleworkable ones become less desirable. As a result, vacancies of the latter type are hard to fill and surge, and vacancies of the former type decline. Among vacant teleworkable jobs, it is the passive ones whose vacancies decrease the most because firms upgrade them more rapidly into active ones to be able to attract high- x workers. The middle panel, which plots match efficiency for these three type of jobs confirms that the desirability of active teleworkable jobs increases significantly, relative to the other types of jobs. Namely, matches with high- x workers can be created with a lower reservation productivity. Finally, the right panel plots newly posted jobs (i.e. the flow of entering, re-entering, or upgrading vacancies) of type $n = 2$ (i.e., active teleworkable). In the first

³⁵More generally, a comparison of the right-panels of Figure 20 and Figure 14 reveals that, because of endogenous frictions, relative wages between active TW and NTW jobs do not equal actual workers' valuation for the job amenity as they would in competitive model, an insight which goes back to Hwang et al. (1998).

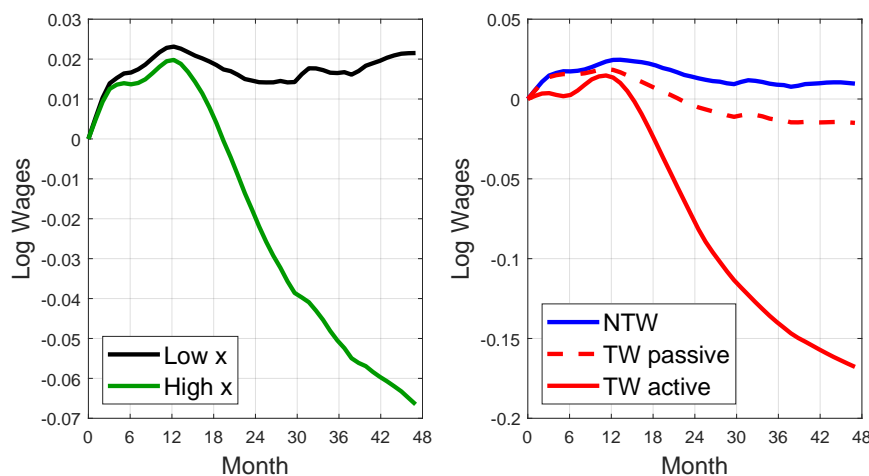


Figure 20: Wages by worker type (left panel), and job type (right panel). Non-teleworkable (NTW) jobs correspond to $n = 0$, TW Passive to $n = 1$, and TW Active to $n = 2$. Log-deviations from initial steady state.

three years of the model transition, the share of these vacancies increases by 10 pct points. Figure 3 in Hansen et al. (2023) shows that the share of online vacancy postings that explicitly offer hybrid or fully remote work rose by a very similar amount between 2020 and 2023.

Dynamics without the job amenity shock. Figure E1 shows the model's best fit to the data when we only allow for shifts in Z^y and Z^b , while keeping the job amenity value fixed at its initial steady-state level. The model matches the unemployment rate well, but it fails in generating the large surge in vacancies, the drop in the job filling rate and the rise in job-to-job transitions. These are the key features of the reallocation process set in motion by the x shock. As a result, the dynamics of the economy in the Beveridge space trace a much flatter relation between unemployment and vacancies relative to the data. Finally, the model lacks a force to pull wages down. As a result of the rebound in productivity and the growth in worker's flow outside option, real wages counterfactually rise above trend in the model.

6.4 Alternative View: Technology-Driven Shift in Remote Work

The view we have taken so far, backed up by the survey evidence of Section 2, is that the pandemic led to a pivot in workers' attitudes toward WFH. An alternative view is that

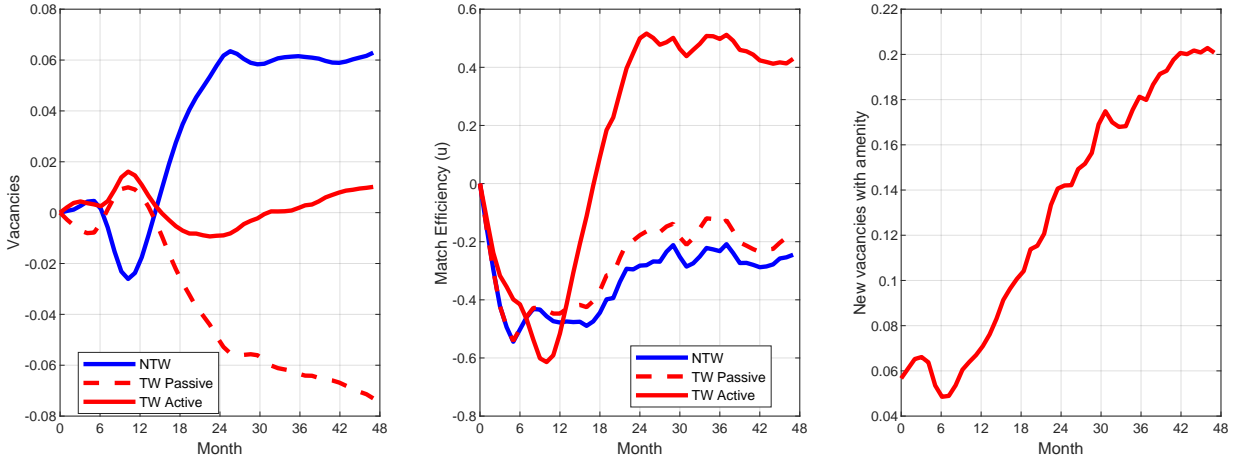


Figure 21: Left panel: Dynamics of vacancy shares by type of job (level deviations from initial steady state). Middle panel: match efficiency by type of job (log-deviations). Right panel: newly created vacancies with amenity as a share of total newly created vacancies. Non-teleworkable (NTW) jobs correspond to $n = 0$, TW Passive to $n = 1$, and TW Active to $n = 2$.

workers' preferences remained unchanged, with the transformation taking place primarily on the firm side as employers devised new ways of producing while offering more flexible arrangements to their workforce.³⁶

From the perspective of our model, we can envision a technology-driven shift in remote work in two ways: either a rise in the share of teleworkable jobs (an aggregate shock to ζ) or an acceleration in the rate at which teleworkable jobs can upgrade and allow their tasks to be performed remotely (an aggregate shock to λ). We have analyzed these shocks in a version of the model with the initial steady state recalibrated to generate a 10% compensating differential for work-from-home which remains stable over time. The model is then estimated on the same time series (as described in Section 6.1) allowing for productivity, labor supply, and one of the technology shocks.

The first type of technological shock has two major shortcomings. First, it implies a massive rise in the employment share of teleworkable jobs (by a factor of two), whereas in the data –and in our model baseline– the increase is only of a few percentage points.³⁷ Second, as depicted in Figure 22, the cross-sectoral patterns induced by a rise in ζ are coun-

³⁶For example, [Barrero et al. \(2021\)](#) discuss the role of the pandemic-driven surge in technological innovations and investments in physical capital which enabled WFH.

³⁷That the employment share on teleworkable occupations has only increased slightly in the data is also visible from Figure 7.

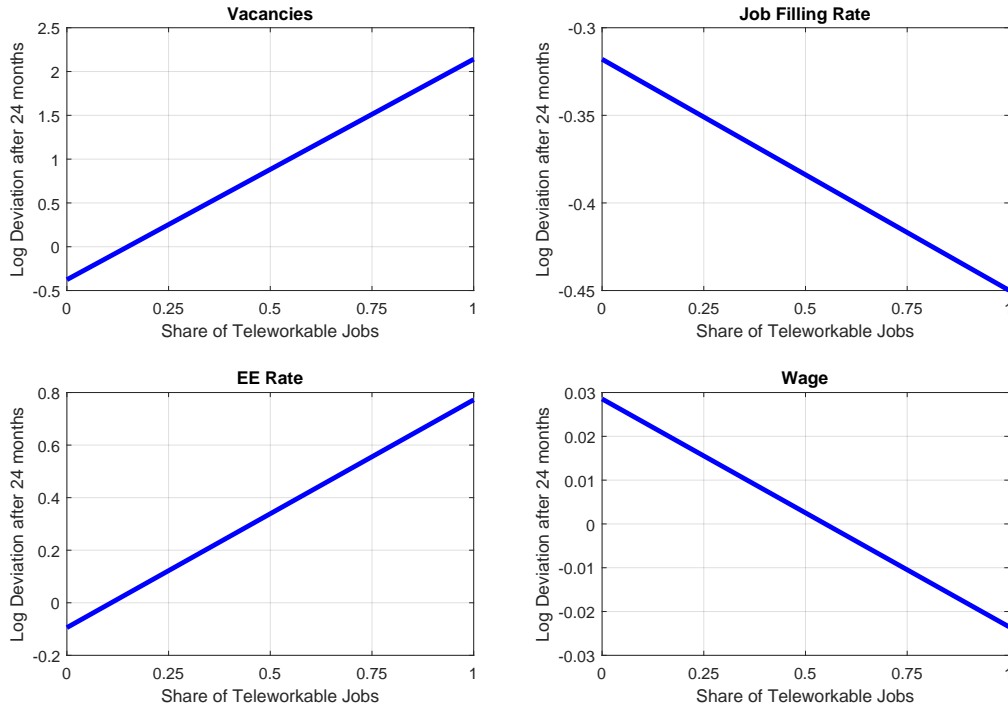


Figure 22: Model counterpart of the cross-sectional evidence of Figure 8 under a shock to the share of teleworkable jobs ζ .

terfactual. This shock expands the relative supply of teleworkable jobs without changing their relative value to workers (as x remains stable), thus it is in the teleworkable sectors that job vacancies grow the most, the job filling rate drops most sharply, and the rise in EE rate is the largest, in contrast with the empirical patterns of Figure 8.

The upgrading shock effectively reduces the cost for employers of offering the job amenity on ongoing matches. Notably, this shock has the virtue of not requiring a significant shift in the teleworkable employment share because it leads to a change of amenity (WFH) status, from passive to active, within teleworkable jobs. Figure 23 summarizes the model equilibrium dynamics in response to this disturbance. The top two panels on the left depict the estimated paths for aggregate shocks to productivity and opportunity cost of work. The critical difference, compared to Figure 14, is that in order to account for the data the model calls for a negative labor supply shock (i.e., a shock that discourages work) which still lingers markedly above trend even 4 years into the recovery. The reason is that the upgrading shock (red line in the Figure) boosts the value of teleworkable vacancies and leads to a surge in vacancy creation paired with a rise in match efficiency. These two forces push down unemployment and expand output. Since the productivity shock is tightly disciplined by the output trajectory, the negative labor supply shock must remain elevated for an extended period to offset these channels. We conclude by noting

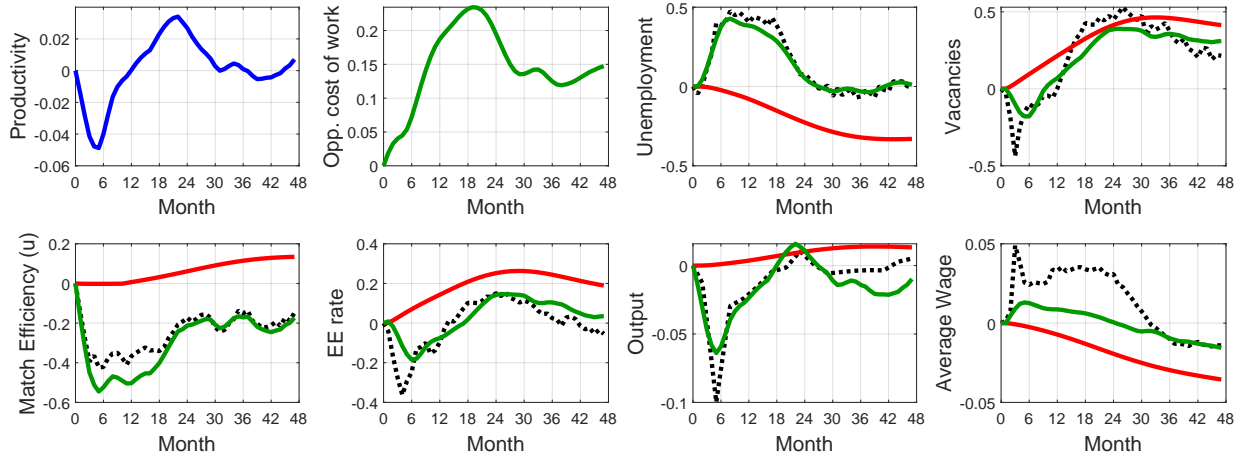


Figure 23: Top left two panels: estimated productivity (blue) and labor supply shock (green). Other panels: decomposition of model's fit of the data (black dotted line) into upgrading shock (red), and upgrading + productivity + labor supply shocks (green). The green line is also the model's fit to the data. Log-deviations from initial steady state.

that the cross-sectional patterns implied by the upgrading shock, depicted in Figure E2 in Appendix E, are also somewhat less stark compared to our baseline.

7 Conclusions

How do frictional labor markets respond to aggregate shifts in the demand and supply of non-pecuniary job amenities? To answer this question, we developed an equilibrium model that combines several building blocks of modern macro-labor: on-the-job search, sunk job creation costs which make jobs vacant when workers quit, non-wage amenities that drive compensating differentials, and sorting between heterogeneous workers and jobs. We applied this framework to interpret the post-pandemic labor market dynamics in the United States. The pandemic was a unique macroeconomic natural experiment because it led to the widespread adoption of a major job amenity, the ability to supply labor services from home. We documented that this shift in work arrangements was accompanied by some historically unique developments in the U.S. labor market, such as a surge in vacancies and quits coupled with stagnant match efficiency and stable unemployment.

In the calibrated model, a shock that raises the value placed by workers on a non-pecuniary job attribute (i.e., work from home) induces a labor reallocation consistent with the key features of the post-pandemic U.S. labor market and wage dynamics. A

technological shock that reduces the cost of supplying the job amenity produces qualitatively similar outcomes. The view that some recessions lead to a spur in worker reallocation across "sectors" goes back at least to [Lilien \(1982\)](#). This traditional view, however, was based on frictional models without on-the-job search and, as a result, was often dismissed because it predicted a counterfactually strongly positive correlation between vacancies and unemployment at business cycle frequencies (e.g. [Abraham and Katz, 1986](#)). We demonstrate that, seen through the lens of state-of-the-art models, reallocation shocks can lead to a rise in the stock of vacancies without higher unemployment as long as the bulk of worker mobility occurs through job-to-job transitions, precisely as occurred in this last episode.

The pandemic was a global shock to labor markets around the world. Going forward, it would be valuable to put the U.S. experience into an international context. The combination of rapid adoption of remote work and unprecedented surges in vacancies and quits seems, at least qualitatively, to have happened in other countries as well, such as U.K. and Australia. At the same time, for example, Japan and South Korea were largely immune to the shift in work arrangements ([Aksoy et al., 2022](#)) and their data do not reveal any significant increase in job vacancies. The framework we have developed here can be used to interpret similarities and divergences between the U.S. labor market experience and those of other countries.

References

- Abraham, K. G. and L. F. Katz (1986). Cyclical unemployment: Sectoral shifts or aggregate disturbances? *Journal of Political Economy* 94(3, Part 1), 507–522.
- Acharya, S. and S. L. Wee (2020). On-the-job search and the productivity-wage gap. *CEPR Discussion Paper No. DP14430*.
- Afrouzi, H., A. Blanco, A. Drenik, and E. Hurst (2024). A theory of how workers keep up with inflation". *NBER Working Paper* 33233.
- Aksoy, C. G., J. M. Barrero, N. Bloom, S. J. Davis, M. Dolls, and P. Zarate (2022). Working from home around the world. *NBER Working Paper* 30446.
- Albrecht, J., C. Carrillo-Tudela, and S. Vroman (2018). On-the-job search with match-specific amenities. *Economics Letters* 162, 15–17.
- Author, D., A. Dube, and A. McGrew (2023). The Unexpected Compression: Competition at Work in the Low Wage Labor Market. *NBER Working Paper* 31010.
- Bai, J. J., E. Brynjolfsson, W. Jin, S. Steffen, and C. Wan (2021). Digital resilience: How work-from-home feasibility affects firm performance. *NBER Working Paper* 28588.
- Barnichon, R. (2010). Building a composite help-wanted index. *Economics Letters* 109(3), 175–178.
- Barrero, J. M., N. Bloom, and S. J. Davis (2021). Why working from home will stick. *NBER Working Paper* 28731.
- Barrero, J. M., N. Bloom, and S. J. Davis (2023a). The evolution of work from home. *Journal of Economic Perspectives* 37(4), 23–49.
- Barrero, J. M., N. Bloom, and S. J. Davis (2023b). Long social distancing. *Journal of Labor Economics* 41(S1), S129–S172.
- Barrero, J. M., N. Bloom, S. J. Davis, B. H. Meyer, and E. Mihaylov (2022). The shift to remote work lessens wage-growth pressures. *NBER Working Paper* 30197.
- Benigno, P. and G. B. Eggertsson (2024). Revisiting the phillips and beveridge curves: Insights from the 2020s inflation surge. *NBER Working Paper* 33095.
- Bick, A. and A. Blandin (2021). Real-time labor market estimates during the 2020 coronavirus outbreak. *Working Paper, Vanderbilt University*.
- Blanchard, O. J. and B. S. Bernanke (2023). What caused the us pandemic-era inflation? *NBER Working Paper* 31417.
- Bloom, N., J. Liang, J. Roberts, and Z. J. Ying (2015). Does working from home work? evidence from a chinese experiment. *The Quarterly Journal of Economics* 130(1), 165–218.
- Bonhomme, S. and G. Jolivet (2009). The pervasive absence of compensating differentials. *Journal of Applied Econometrics* 24(5), 763–795.

- Boppart, T., P. Krusell, and K. Mitman (2018). Exploiting mit shocks in heterogeneous-agent economies: the impulse response as a numerical derivative. *Journal of Economic Dynamics and Control* 89, 68–92.
- Chen, Y., P. Cortes, G. Kosar, J. Pan, and B. Zafar (2023). The impact of covid-19 on workers' expectations and preferences for remote work. In *AEA Papers and Proceedings*, Volume 113, pp. 556–561.
- Coles, M. G. and A. M. Kelishomi (2018). Do job destruction shocks matter in the theory of unemployment? *American Economic Journal: Macroeconomics* 10(3), 118–36.
- Crump, R., S. Eusepi, M. Giannoni, and A. Şahin (2019). A unified approach to measuring u^* . *NBER Working Paper* 25930.
- Cullen, Z. B., B. Pakzad-Hurson, and R. Perez-Truglia (2025). Home sweet home: How much do employees value remote work? *NBER Working Paper* 33383.
- Daly, M. C., B. Hobijn, A. Şahin, and R. G. Valletta (2012). A search and matching approach to labor markets: Did the natural rate of unemployment rise? *Journal of Economic Perspectives* 26(3), 3–26.
- Davis, S., R. J. Faberman, and J. Haltiwanger (2013). The establishment-level behavior of vacancies and hiring. *The Quarterly Journal of Economics* 26(3), 3–26.
- Davis, S. J. (2024). Extraordinary labor market developments and the 2022-23 disinflation. *NBER Working Paper* 32584.
- Dingel, J. I. and B. Neiman (2020). How many jobs can be done at home? *Journal of Public Economics* 189, 1–8.
- Elsby, M., A. Gottfries, R. Michaels, and D. Ratner (2022). Vacancy chains. Working Paper 22-23, Federal Reserve Bank of Philadelphia.
- Emanuel, N. and E. Harrington (2024). Working remotely? selection, treatment, and the market for remote work. *American Economic Journal: Applied Economics* 16(4), 528–559.
- Faberman, R. J., A. I. Mueller, A. Şahin, and G. Topa (2022). Job search behavior among the employed and non-employed. *Econometrica* 90(4), 1743–1779.
- Fujita, S., G. Moscarini, and F. Postel-Vinay (2024). Measuring employer-to-employer reallocation. *American Economic Journal: Macroeconomics* 16(3), 151.
- Fujita, S. and G. Ramey (2007). Job matching and propagation. *Journal of Economic Dynamics and Control* 31(11), 3671–3698.
- Gavazza, A., S. Mongey, and G. L. Violante (2018). Aggregate recruiting intensity. *American Economic Review* 108(8), 2088–2127.
- Gittleman, M. (2022). The great resignation in perspective. *Monthly Labor Review*, U.S. Bureau of Labor Statistics, November 2022.

- Guerreiro, J., J. Hazell, C. Lian, and C. Patterson (2024). Why do workers dislike inflation? wage erosion and conflict costs. *NBER Working Paper* 32956.
- Hall, R. E. and M. Kudlyak (2022). The unemployed with jobs and without jobs. *Labour Economics* 79, 102244.
- Hall, R. E. and A. I. Mueller (2018). Wage dispersion and search behavior: The importance of nonwage job values. *Journal of Political Economy* 126(4), 1594–1637.
- Hall, R. E. and S. Schulhofer-Wohl (2018). Measuring job-finding rates and matching efficiency with heterogeneous job-seekers. *American Economic Journal: Macroeconomics* 10(1), 1–32.
- Hansen, S., P. J. Lambert, N. Bloom, S. J. Davis, R. Sadun, and B. Taska (2023). Remote Work across Jobs, Companies, and Space. *NBER Working Paper* 31007.
- Hershbein, B. J. (2017). The new hires quality index: A wage metric for newly hired workers. *Working Paper*, W.E. Upjohn Institute for Employment Research.
- Hornstein, A., P. Krusell, and G. L. Violante (2007). Technology-policy interaction in frictional labour markets. *The Review of Economic Studies* 74(4), 1089–1124.
- Hwang, H., D. T. Mortensen, and W. R. Reed (1998). Hedonic wages and labor market search. *Journal of Labor Economics* 16(4), 815–847.
- Lamadon, T., J. Lise, C. Meghir, and J.-M. Robin (2024). Labor market matching, wages, and amenities. *NBER Working Paper* 32687.
- Le Barbanchon, T., R. Rathelot, and A. Roulet (2021). Gender differences in job search: Trading off commute against wage. *The Quarterly Journal of Economics* 136(1), 381–426.
- Lilien, D. M. (1982). Sectoral shifts and cyclical unemployment. *Journal of Political Economy* 90(4), 777–793.
- Lindenlaub, I. and F. Postel-Vinay (2023). Multidimensional sorting under random search. *Journal of Political Economy* 131(12), 3497–3539.
- Lise, J. and J.-M. Robin (2017). The macrodynamics of sorting between workers and firms. *American Economic Review* 107(4), 1104–35.
- Mas, A. (2025). Non-wage amenities. *NBER Working Paper* 33643.
- McKay, A. and J. F. Wieland (2021). Lumpy durable consumption demand and the limited ammunition of monetary policy. *Econometrica* 89(6), 2717–2749.
- Mercan, Y. and B. Schoefer (2020, March). Jobs and matches: Quits, replacement hiring, and vacancy chains. *American Economic Review: Insights* 2(1), 10124.
- Moscarini, G. and F. Postel-Vinay (2023). The job ladder: Inflation vs. reallocation. *NBER Working Paper* 31466.

- Mukoyama, T., C. Patterson, and A. Şahin (2018). Job search behavior over the business cycle. *American Economic Journal: Macroeconomics* 10(1), 190–215.
- Nosal, E. and P. Rupert (2007). How amenities affect job and wage choices over the life cycle. *Review of Economic Dynamics* 10(3), 424–443.
- Petrongolo, B. and C. A. Pissarides (2001). Looking into the black box: A survey of the matching function. *Journal of Economic Literature* 39(2), 390–431.
- Petrosky-Nadeau, N. and L. Zhang (2021). Unemployment crises. *Journal of Monetary Economics* 117, 335–353.
- Pilossoph, L. and J. M. Ryngaert (2024). Job search, wages, and inflation. *NBER Working Paper* 33042.
- Postel-Vinay, F. and J.-M. Robin (2002). The distribution of earnings in an equilibrium search model with state-dependent offers and counteroffers. *International Economic Review* 43(4), 989–1016.
- Qiu, X. (2024). Vacant jobs. *Working Paper, Peking University*.
- Reiter, M. (2018). Comments on exploiting MIT shocks in heterogeneous-agent economies: The impulse response as a numerical derivative by T. Boppart, P. Krusell and K. Mitman. *Journal of Economic Dynamics and Control* 89, 93–99.
- Rosen, S. (1986). The theory of equalizing differences. *Handbook of Labor Economics* 1, 641–692.
- Sahin, A., J. Song, G. Topa, and G. L. Violante (2014). Mismatch unemployment. *American Economic Review* 104(11), 3529–3564.
- Sedláček, P. and C. Shi (2024). Macroeconomic impact of the remote work revolution. *Working Paper, University of Oxford*.
- Sorkin, I. (2018). Ranking firms using revealed preference. *The Quarterly Journal of Economics* 133(3), 1331–1393.

Appendix

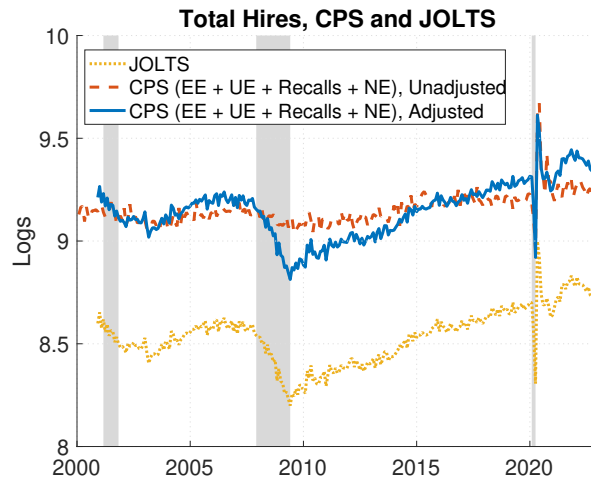
A Adjusting CPS and JOLTS hires in levels and cyclicity

The Current Population Survey (CPS) and Job Openings and Labor Turnover Survey (JOLTS) provide us with monthly measures of hires from the worker and firm side, respectively. In the CPS, hires in month t are defined as the sum of all workers who make flows into employment in month t from the state of employment in a different firm, unemployment (including temporary layoffs), or non-participation in month $t - 1$. In the JOLTS, hires are defined as "any addition to an establishment's payroll, including newly hired and rehired employees.". In principle, both data sources capture total hires and should provide us with comparable measures. In practice, there is a discrepancy between these measures in levels and cyclicity. Figure A1 plots the CPS and JOLTS hires and shows that CPS hires are less cyclical and higher in levels compared to JOLTS hires. (The difference in levels between CPS and JOLTS has also been pointed out by [Fujita et al. \(2024\)](#) (focus on separations) and [Hershbein \(2017\)](#)).

Throughout the paper, we adjust the total hires to match the JOLTS cyclicity and CPS levels. We re-scale all sources of hires in the CPS by adjusting for them for the cyclicity and levels factors defined below:

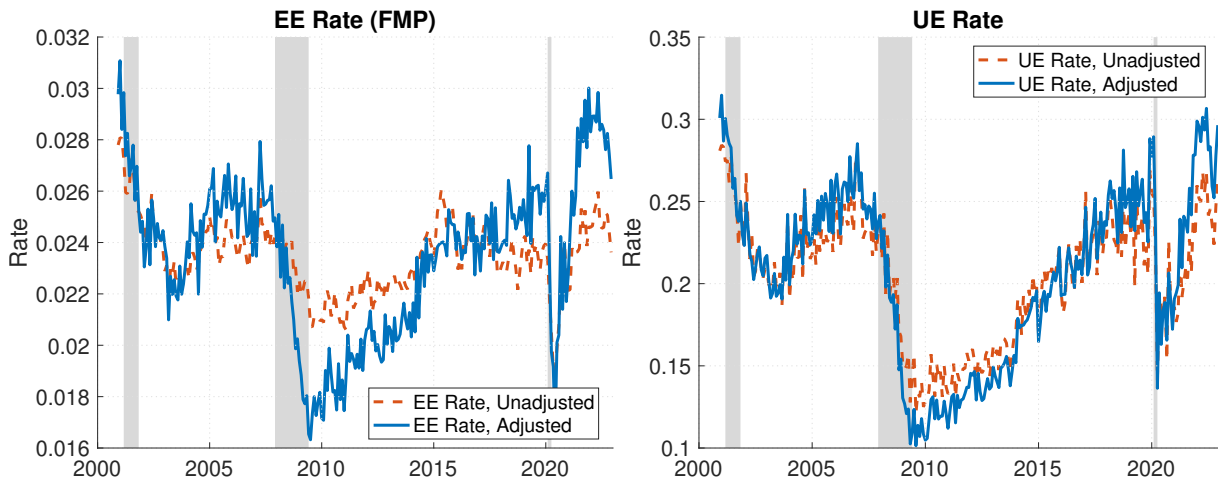
$$\text{Hires Cyclicity Factor}_t = \frac{Hires_t^{JOLTS}}{UE_t^{CPS} + NE_t^{CPS} + EE_t^{CPS} + Recalls_t^{CPS}}$$
$$\text{Hires Level Factor} = \frac{\overline{UE}^{CPS} + \overline{NE}^{CPS} + \overline{EE}^{CPS} + \overline{Recalls}^{CPS}}{\overline{Hires}^{JOLTS}}$$

We adjust the flow of UE hires, EE hires, and stock of the unemployed by expressing them as products of the hires cyclicity and level factors.



Source: CPS, JOLTS, and authors' calculations.

Figure A1: Total Hires from the CPS and JOLTS. The CPS hires have been adjusted for JOLTS cyclicalities and CPS levels.



Source: CPS, JOLTS, and authors' calculations.

Figure A2: UE rate and [Fujita et al. \(2024\)](#)-based EE rate. Adjusted for JOLTS cyclicalities and CPS levels.

B Variable Definitions

- Unemployment Rate: Number of unemployed (excluding those on temporary layoffs) expressed as a fraction of the sum of employed and unemployed (excluding those on temporary layoffs).
- Vacancy Rate: Number of job openings expressed as a fraction of the sum of employees and job openings. Obtained from the JOLTS.
- Labor Market Tightness: Vacancies/Unemployed (excluding those on temporary layoffs)
- Beveridge Curve: Vacancy Rate plotted against Unemployment Rate
- Job Finding Rate: $(UE \text{ hires} + EE \text{ hires}) / \text{Job seekers}$ ($U + s * E$) where $s = 0.78$.
- Job Filling Rate: $(UE \text{ hires} + EE \text{ hires}) / \text{Vacancies}$
- Quits Rate: Quits/Employed. Obtained from the JOLTS.
- EE Rate: EE hires/Employed.
- UE Rate: UE hires/Unemployed (excluding those on temporary layoffs)

C Additional tables and figures

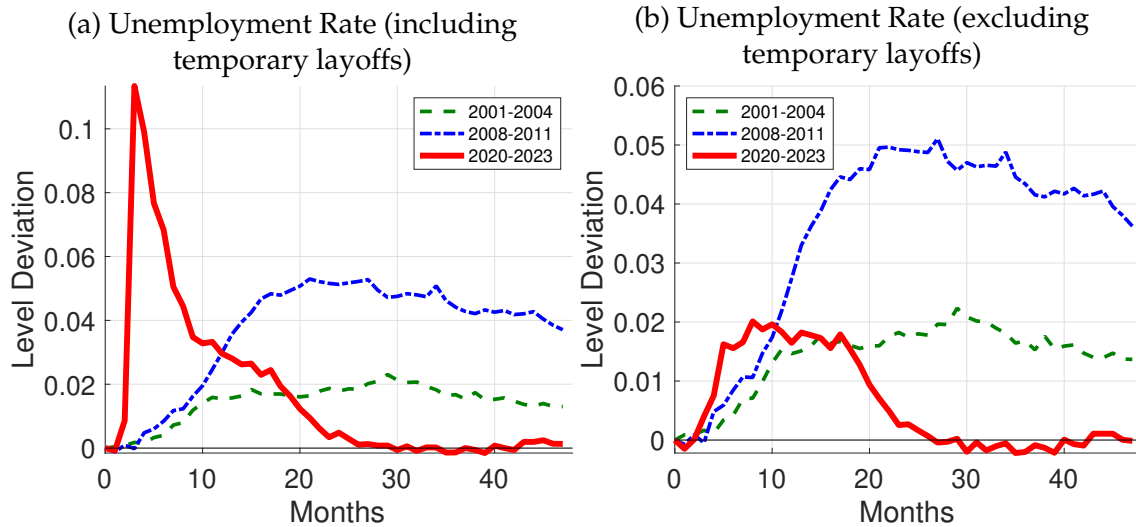


Figure C1: Unemployment rate with and without temporary layoffs in the past three business cycles

Notes: CPS, and authors' calculations. Y-axis shows level deviation in the unemployment rate including (panel a) and excluding (panel b) workers on temporary layoffs in 2001-2004, 2008-2011, and 2020-2023 periods. The initial values are normalized to zero in January 2001, 2008, and 2020.

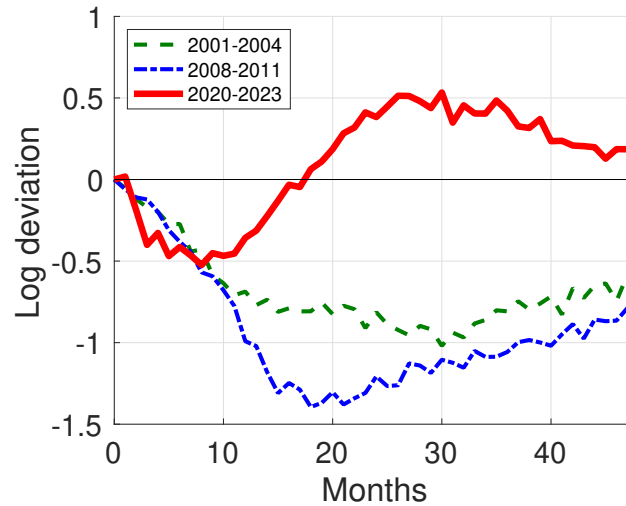


Figure C2: Vacancy-to-unemployment ratio

Notes: CPS, JOLTS, and authors' calculations. Y-axis shows log deviation in labor market tightness defined as vacancies/unemployed in 2001-2004, 2008-2011, and 2020-2023 periods. The values are normalized to zero for January 2001, 2008, and 2020.

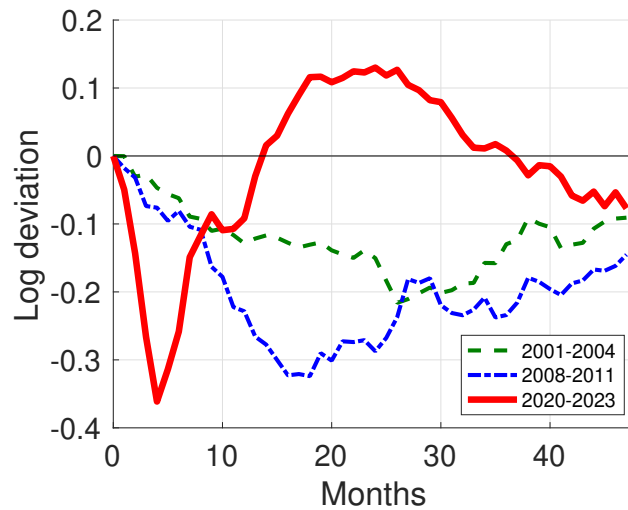


Figure C3: Job Finding Rate, All jobseekers

Notes: CPS, JOLTS, and authors' calculations. The values are normalized to zero for January 2001, 2008, and 2020. Job finding rate is defined as total hires from employment and unemployment as a fraction of all jobseekers, and expressed as a 3-month centered moving average. The relative weight on employed jobseekers is 0.78 based on [Faberman et al. \(2022\)](#). Total hires have been constructed to reflect CPS levels and for JOLTS cyclicalities as described in [Appendix A](#).

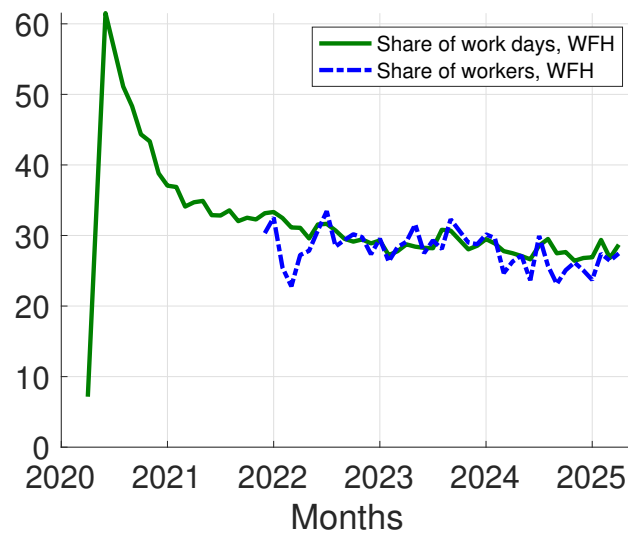


Figure C4: Work from home work days and workers

Notes: The green line plots the percent of full paid working days spent on work from home. The first value uses the 2019 American Time Use Survey, whereas the rest of the series uses Survey of Working Arrangements and Attitudes (SWAA). The blue line plots the percent of full-time wage and salary workers in hybrid work arrangements from the SWAA. Source: Work from home statistics from [Barrero, Bloom, and Davis \(2021\)](#).



Figure C5: Labor Market Outcomes by Goods vs. Services Sectors

Notes: CPS, JOLTS and author's calculations. Goods sector includes construction, manufacturing and mining, while services sector includes arts and accommodation, health and education, information and finance, professional services, real estate, trade and transport, and other services.

	(1)	(2)	(3)	(4)	(5)	(6)
	2020m1-2023m1		2008m1-2011m1		2001m1-2004m1	
	<i>v</i>	<i>jfr</i>	<i>v</i>	<i>jfr</i>	<i>v</i>	<i>jrf</i>
Log Quits Rate	0.407*** (0.035)	0.294*** (0.039)	0.302*** (0.025)	0.435*** (0.031)	0.370*** (0.020)	0.456*** (0.026)
Year FE	Y	Y	Y	Y	Y	Y
N	629	629	629	629	629	629
R ²	0.620	0.388	0.320	0.217	0.304	0.242

Table C1: Regressions: Vacancies, Job Filling and Quits

Notes: JOLTS, 2001m1-2023m1, seasonally adjusted. *v* denotes log vacancy rate, and *jfr* denotes log job filling rate defined as hires divided by vacancies. Robust standard errors in parenthesis. * p<0.10, ** p<0.05, *** p<0.01.

Table C2: Industry labels for Figure 9

Label	NAICS 3-digit name	NAICS 3-digit code
utl	Utilities	221
cons1	Construction of Buildings	236
cons2	Heavy and Civil Engineering Construction	237
cons3	Specialty Trade Contractors	238
mfg1	Food Manufacturing	311
mfg2	Beverage and Tobacco Product Manufacturing	312
mfg3	Textile Mills	313
mfg4	Textile Product Mills	314
mfg5	Apparel Manufacturing	315
mfg6	Leather and Allied Product Manufacturing	316
mfg7	Wood Product Manufacturing	321
mfg8	Paper Manufacturing	322
mfg9	Printing and Related Support Activities	323
mfg10	Petroleum and Coal Products Manufacturing	324
mfg11	Chemical Manufacturing	325
mfg12	Plastics and Rubber Products Manufacturing	326
mfg13	Nonmetallic Mineral Product Manufacturing	327
mfg14	Primary Metal Manufacturing	331

(Table C2 continued)

Label	NAICS 3-digit name	NAICS 3-digit code
mfg15	Fabricated Metal Product Manufacturing	332
mfg16	Machinery Manufacturing	333
mfg17	Computer and Electronic Product Manufacturing	334
mfg18	Electrical Equipment, Appliance, and Component Manufacturing	335
mfg19	Transportation Equipment Manufacturing	336
mfg20	Furniture and Related Product Manufacturing	337
mfg21	Miscellaneous Manufacturing	339
whole1	Merchant Wholesalers, Durable Goods	423
whole2	Merchant Wholesalers, Nondurable Goods	424
whole3	Wholesale Electronic Markets and Agents and Brokers	425
retail1	Motor Vehicle and Parts Dealers	441
retail2	Building Material and Garden Equipment and Supplies Dealers	444
retail3	Food and Beverage Stores	445
retail4	Furniture, Home Furnishings, Electronics and Appliance Stores	449
retail5	General Merchandise Stores	455
retail6	Health and Personal Care Stores	456
retail7	Gasoline Stations	457
retail8	Clothing and Clothing Accessories Stores	458
retail9	Sporting Goods, Hobby, Musical Instrument, and Book Stores	459
trans1	Air Transportation	481
trans2	Water Transportation	483
trans3	Truck Transportation	484
trans4	Transit and Ground Passenger Transportation	485
trans5	Pipeline Transportation	486
trans6	Scenic and Sightseeing Transportation	487
trans7	Support Activities for Transportation	488
trans8	Postal Service (federal government)	491
trans9	Couriers and Messengers	492
trans10	Warehousing and Storage	493
info1	Motion Picture and Sound Recording Industries	512

(Table C2 continued)

Label	NAICS 3-digit name	NAICS 3-digit code
info2	Publishing Industries (except Internet)	513
info3	Broadcasting (except Internet)	516
info4	Telecommunications	517
info5	Data Processing, Hosting, and Related Services	518
info6	Other Information Services	519
fin1	Monetary Authorities-Central Bank	521
fin2	Credit Intermediation and Related Activities	522
fin3	Securities, Commodity Contracts, and Other Financial Investments and Related Activities	523
fin4	Insurance Carriers and Related Activities	524
fin5	Funds, Trusts, and Other Financial Vehicles	525
realest1	Real Estate	531
realest2	Rental and Leasing Services	532
realest3	Lessors of Nonfinancial Intangible Assets (except Copyrighted Works)	533
prof	Professional, Scientific, and Technical Services	541
mgmt	Management of Companies and Enterprises	551
admin1	Administrative and Support Services	561
admin2	Waste Management and Remediation Services	562
edu	Educational Services	611
health1	Ambulatory Health Care Services	621
health2	Hospitals	622
health3	Nursing and Residential Care Facilities	623
health4	Social Assistance	624
arts1	Performing Arts, Spectator Sports, and Related Industries	711
arts2	Museums, Historical Sites, and Similar Institutions	712
arts3	Amusement, Gambling, and Recreation Industries	713
acc1	Accommodation	721
acc2	Food Services and Drinking Places	722
othser1	Repair and Maintenance	811
othser2	Personal and Laundry Services	812
othser3	Religious, Grantmaking, Civic, Professional, and Similar Organizations	813

D Model Derivations

This appendix complements the theoretical model of Section 3. It is organized as follows. Sections D.1 obtains wages, given the assumed wage setting protocol. Section D.2 describes the upgrading decisions. Section D.3 derives the Bellman equations for firm and worker. Building on these assumptions and equations, Section D.4 shows that the gross surplus equation can be written as in equation 10 in the main text. Section D.5 derives the values for actively recruiting and dormant vacancies. Section D.6 obtains the law of motion for the stocks of employed workers, unemployed workers, and vacancies. Section D.7 defines endogenous match efficiency in the model. Section D.8 defines a perfect foresight equilibrium for our economy, and Section D.9 illustrates our numerical solution algorithm.

It is useful to start with some notation. Let $J_t, W_t, \Omega_t, \tilde{\Omega}_t, U_t$ denote, respectively, the value of a filled job, an employed worker, an actively recruiting vacancy, a dormant vacancy, and an unemployed worker at time t . Let $S_t := J_t + W_t - U_t$ be the gross surplus of a match, i.e. the surplus without netting out the firm outside option. All equations we derive below refer to the case where boundary conditions are non-binding.

D.1 Wage Determination

Let ϕ_t denote the wage paid to the worker as a function of the relevant individual state variables. To describe how wages are determined in our model, we have six different cases to consider:

1. When an unemployed worker of type x meets a vacancy of type n , and the match value y is observed, the match is created if $J_t(\phi_t^u, x, y, n) > \Omega_t(n)$. Because of the take-or-leave (ToL) protocol, the wage is set to the value $\phi_t^u(x, y, n)$ that sets the worker value to their outside option, or

$$W_t(\phi_t^u, x, y, n) = U_t(x). \quad (\text{E1})$$

Since $S_t(x, y, n) = J_t(\phi_t^u, x, y, n) + W_t(\phi_t^u, x, y, n) - U_t(x)$, the value of a firm can be expressed as

$$J_t(\phi_t^u, x, y, n) = S_t(x, y, n), \quad (\text{E2})$$

i.e. due to the ToL protocol, upon hiring a worker from unemployment, the firm initially receives all the surplus from the relationship. Equation (E2) determines the wage $\phi^u(x, y, n)$.

2. When an employed worker of type x on a job (y, n) meets a firm (y', n') and $S_t(x, y', n') - \Omega_t(n') > S_t(x, y, n) - \tilde{\Omega}_t(n)$, the worker moves to the new firm (y', n') because the poach-

ing firm can always pay more than the current one can match. At the time of the transition, the worker's outside option is to extract the whole surplus at the previous match. At the new match, the worker therefore receives value

$$W_t(\phi_t^q, x, y', n') - U_t(x) = S_t(x, y, n) - \tilde{\Omega}_t(n) \quad (\text{E3})$$

This equation determines the wage $\phi_t^q(x, y, n, y', n')$ upon the job-to-job transition. As a result, the poaching firm value becomes

$$J_t(\phi_t^q, x, y', n') = S_t(x, y', n') - [S_t(x, y, n) - \tilde{\Omega}_t(n)] \quad (\text{E4})$$

3. When an employed worker of type x on firm (y, n) meets a firm (y', n') and $W_t(w, n, x, y) - U_t(x) < S_t(x, y', n') - \Omega_t(n') \leq S_t(n, x, y) - \tilde{\Omega}_t(n)$, the worker stays with their current employer, but can use this outside offer to improve their position within the current firm. In this case, the incumbent firm makes a ToL offer to the worker which is just enough to make them indifferent between staying and quitting and thus retains the worker:

$$W_t(\phi_t^r, x, y, n) - U_t(x) = S_t(x, y', n') - \Omega_t(n') \quad (\text{E5})$$

This also determines the new retention wage $\phi_t^r(x, y, n, y', n')$. In this case, the current firm value drops to

$$J_t(\phi_t^r, x, y, n) = S_t(x, y, n) - [S_t(x, y', n') - \Omega_t(n')]. \quad (\text{E6})$$

4. Whenever an employed worker of type x on firm (y, n) meets a firm of type (y', n') and $S_t(x, y, n) - \tilde{\Omega}_t(n) > W_t(w, x, y, n) - U_t(x) \geq S_t(x, y, n') - \Omega_t(n')$, the worker has nothing to gain from the outside offer. The worker does not quit and their wage remains the same.
5. Even though we consider only MIT shocks + transition dynamics, such an unexpected aggregate shock can also lead to renegotiation at impact or during the transition. If, at any point under the old contract w ,

$$W_t(w, x, y) - U_t(x) < 0, \quad \text{but } S_t(x, y, n) - \tilde{\Omega}_t(n) \geq 0$$

then the wage is set to ϕ_t^+ just enough to avoid quitting, i.e.

$$W_t(\phi_t^+, x, y, n) - U_t(x) = 0 \quad (\text{E7})$$

Equation (E7) also determines $\phi_t^+(x, y, z)$ after the shock. The firm value raises to

$$J_t(\phi_t^+, x, y, n) = S_t(x, y, n) \quad (\text{E8})$$

6. The reverse situation occurs when, along the transition, the wage is too high and it is the firm that threatens to fire the worker, i.e.

$$J_t(w, x, y, n) < \tilde{\Omega}_t(n), \quad \text{but } S_t(x, y, n) \geq \tilde{\Omega}_t(n)$$

Since $J_t(w, x, y, n) = S_t(a, x, y) - [W_t(w, x, y, n) - U_t(x)]$, the value of the firm will be raised just enough to avoid a layoff

$$J_t(\phi_t^-, x, y, n) = \tilde{\Omega}_t(n) \quad (\text{E9})$$

and the new wage ϕ^- will satisfy

$$W_t(\phi_t^-, x, y, n) - U_t(x) = S_t(x, y, n) - \tilde{\Omega}_t(n) \quad (\text{E10})$$

an equation which determines $\phi_t^-(x, y, n)$.

7. We assume that worker-firm matches commit to upgrading –denoted by the symbol \uparrow – if and only if it maximizes the match's joint surplus $S_t(x, y, n)$. We further assume that wages stay fixed upon upgrading, unless one of the two boundary conditions, $J_t(w, x, y, n) \geq \tilde{\Omega}_t(n)$ or $W_t(w, x, y) \geq U_t(x)$, binds after the upgrade. If a boundary condition binds, the wage is renegotiated to make the boundary condition hold with equality, as described above. We can thus write compactly

$$\phi_t^\uparrow(w, x, y, 2) = \min\{\max\{w, \phi_t^+(x, y, 2)\}, \phi_t^-(x, y, 2)\}. \quad (\text{E11})$$

D.2 Upgrading

Upgrading opportunities arise with rate π for filled jobs and with rate $\vartheta\pi$ for vacant ones. In what follows, we will consider first the case where upgrading occurs during an ongoing employment relationship. At the end of the section, we discuss the case of upgrading of vacant jobs.

D.2.1 Upgrading for Ongoing Matches

Upon an upgrading opportunity, the upgrading cost c is drawn from a $U[0, \frac{\pi}{\lambda}]$ distribution (i.e. a distribution with cdf $G(c) = \frac{\lambda}{\pi}c$ for $c \in [0, \frac{\pi}{\lambda}]$). Let $S(x, y, 2)$ be the gross surplus of an upgraded (active teleworkable) job and $S(x, y, 1)$ be the gross surplus of a non-upgraded (passive teleworkable) job. Define

$$\Delta_{S_t} = \mathbb{I}_{\{n=1\}} \max\{0, S_t(x, y, 2) - S_t(x, y, 1)\}$$

The firm upgrades if and only if $S_t(x, y, 2) - c \geq S_t(x, y, 1) \iff c \leq \Delta_{S_t}$. Thus, the probability of upgrading conditional on an upgrading opportunity equals

$$\Pr(\uparrow) = \Pr(c \leq \Delta_{S_t}) = G(\Delta_{S_t}) = \frac{\lambda \Delta_{S_t}}{\pi}$$

Note that $\frac{\lambda \Delta_{S_t}}{\pi} < 1$ as long as π is sufficiently large. We will consider the limit $\pi \rightarrow \infty$ which ensures that this is always true. This will mean that cost considerations, rather than exogenous restrictions, always govern the rate of upgrading.

The unconditional rate of upgrading by the firm is

$$\pi \Pr(\uparrow) = \lambda \Delta_{S_t}$$

which is independent of π . Furthermore,

$$\begin{aligned} \mathbb{E}[c | c \leq \Delta_{S_t}] &= G(\Delta_{S_t})^{-1} \int_0^{\Delta_{S_t}} c dG(c) \\ &= G(\Delta_{S_t})^{-1} \int_0^{\Delta_{S_t}} \frac{\lambda}{\pi} c dc \\ &= G(\Delta_{S_t})^{-1} \left(\frac{\lambda}{\pi} \frac{1}{2} \Delta_{S_t}^2 \right) \\ &= \frac{1}{2} \Delta_{S_t} \end{aligned}$$

Consider now the Bellman equation for gross surplus. This equation takes the form

$$rS_t(x, y, 1) = \dots + \pi (\mathbb{E}[\max\{S_t(x, y, 2) - c, S_t(x, y, 1)\}] - S_t(x, y, 1))$$

which can be written as

$$\begin{aligned} rS_t(x, y, 1) &= \dots + \pi \left(\Pr(\uparrow) \mathbb{E}[S_t(x, y, 2) - c | c \leq \Delta_{S_t}] + (1 - \Pr(\uparrow)) S_t(x, y, 1) - S_t(x, y, 1) \right) \\ &= \dots + \pi \Pr(\uparrow) \mathbb{E}[\Delta_{S_t} - c | c \leq \Delta_{S_t}] \\ &= \dots + \lambda \Delta_{S_t} (\Delta_{S_t} - \frac{1}{2} \Delta_{S_t}) \\ &= \dots + \frac{\lambda}{2} \Delta_{S_t}^2 \end{aligned}$$

which shows that the value of π is irrelevant for these Bellman equations as well.

Finally, we turn to individual worker and firm value functions. Using the rules from the wage setting protocol outlined above, the decision to upgrade is taken jointly, but individual values may

go up or down as a result. Thus, denoting

$$\Delta_{W_t} = \mathbb{I}_{\{n=1\}} (W_t(\phi_t^\uparrow(w, x, y, 2), x, y, 2) - W_t(w, x, y, 1))$$

and

$$\Delta_{J_t} = \mathbb{I}_{\{n=1\}} (J_t(\phi_t^\uparrow(w, x, y, 2), x, y, 2) - J_t(w, x, y, 1))$$

we have

$$\begin{aligned} rW_t(w, x, y, 1) &= \dots + \pi \left(\Pr(\uparrow) \mathbb{E}[W_t(w, x, y, 2) | c \leq \Delta_{S_t}] + (1 - \Pr(\uparrow)) W_t(w, x, y, 1) - W_t(w, x, y, 1) \right) \\ &= \dots + \pi \Pr(\uparrow) \Delta_{W_t} \\ &= \dots + \lambda \Delta_{S_t} \cdot \Delta_{W_t} \end{aligned}$$

and

$$\begin{aligned} rJ_t(w, x, y, 1) &= \dots + \pi \left(\Pr(\uparrow) \mathbb{E}[J_t(w, x, y, 2) - c | c \leq \Delta_{S_t}] + (1 - \Pr(\uparrow)) J_t(w, x, y, 1) - J_t(w, x, y, 1) \right) \\ &= \dots + \pi \Pr(\uparrow) \mathbb{E}[\Delta_{J_t} - c | c \leq \Delta_{S_t}] \\ &= \dots + \lambda \Delta_{S_t} (\Delta_{J_t} - \frac{1}{2} \Delta_{S_t}) \end{aligned}$$

These expressions are likewise independent of π . Recall that this result, which allows us to save on a parameter, depends on the functional form assumption for $G(c)$.

D.2.2 Upgrading for Vacancies

An actively recruiting vacant job of type $n = 1$ has the opportunity to upgrade at rate $\vartheta\pi$, and it does so if $\Omega_t(2) - c \geq \Omega_t(1)$, where $c \sim G$. We assume that dormant vacancies cannot upgrade.

In line with our notation for the case of ongoing matches, we let

$$\Delta_{\Omega_t} = \mathbb{I}_{\{n=1\}} \max\{0, \Omega_t(2) - \Omega_t(1)\}.$$

By following analogous steps to the case of ongoing matches, it is easy to show that the value of a vacancy takes the form

$$r\Omega_t(1) = \dots + \frac{\vartheta\lambda}{2} \Delta_{\Omega_t}^2$$

D.2.3 Upgrading Sets

For the definition of equilibrium of Section D.8, it is useful to define upgrading sets for ongoing matches and vacancies, respectively

$$U_S(x, y) = \{c : S_t(x, y, 2) - S(x, y, 1) \geq c\} \quad (\text{E12})$$

$$U_\Omega = \{c : \Omega_t(2) - \Omega_t(1) \geq c\} \quad (\text{E13})$$

D.3 Match Value

The firm's value of a match at date t between a worker of type x and a job of type n which produces output y where the worker is paid a wage w is given by

$$\begin{aligned} (r + \delta + sp_t)J_t(w, x, y, n) &= Z_t^y y - w + \delta \tilde{\Omega}_t(n) \\ &+ sp_t \underbrace{\sum_{(n', y') \in \mathcal{Q}_t(x, y, n)} \tilde{\Omega}_t(n) \cdot f(y') \cdot \left(\frac{v_t(n')}{v_t}\right)}_{\text{worker quits to better job}} \\ &+ sp_t \underbrace{\sum_{(n', y') \in \mathcal{R}_t(x, y, n)} J_t(\phi_t^r, x, y, n) \cdot f(y') \cdot \left(\frac{v_t(n')}{v_t}\right)}_{\text{worker is retained with higher wage}} \\ &+ sp_t \underbrace{\sum_{(n', y') \in \mathcal{N}_t(x, y, n)} J_t(w, x, y, n) \cdot f(y') \cdot \left(\frac{v_t(n')}{v_t}\right)}_{\text{worker meets worse firm}} \\ &+ \underbrace{\lambda \Delta_{S_t}(\Delta_{J_t} - \frac{1}{2} \Delta_{S_t})}_{\text{job upgrades}} \\ &+ \partial_t J_t(w, x, y, n) \end{aligned} \quad (\text{E14})$$

where

$$\mathcal{Q}_t(x, y, n) = \{(y', n') : S_t(x, y', n') - \Omega_t(n') > S_t(x, y, n) - \tilde{\Omega}_t(n)\} \quad (\text{E15})$$

and

$$\mathcal{R}_t(x, y, n) = \{(y', n') : W_t(w, x, y, n) - U_t(x) < S_t(x, y', n') - \Omega_t(n') \leq S_t(x, y, n) - \tilde{\Omega}_t(n)\} \quad (\text{E16})$$

are sets of the draws of job offers (y', n') which trigger respectively a quit and a renegotiation. The set

$$\mathcal{N}_t(x, y, n) = \{(y', n') : S_t(x, y, n) - \tilde{\Omega}_t(a) > W_t(w, x, y, n) - U_t(x) \geq S_t(x, y', a') - \Omega_t(n')\} \quad (\text{E17})$$

is the set of firms that attempt to poach but are so low-productivity that no renegotiation is triggered.

Unemployed and Employed Workers The value of unemployment for a worker of type x is

$$(r + p_t)U_t(x) = Z_t^b b + p_t \sum_{n,y} \left[\underbrace{\mathbb{I}_{\{x \in \mathcal{H}_t(y,n)\}} W_t(\phi_t^u, x, y, n)}_{\text{successful contacts}} + \underbrace{\mathbb{I}_{\{x \notin \mathcal{H}_t(y,n)\}} U_t(x)}_{\text{failed contacts}} \right] \left(\frac{v_t(n)}{v_t} \right) f(y) + \partial_t U_t(x)$$

where

$$\mathcal{H}_t(y, n) = \{x : S_t(x, y, n) > \Omega_t(n)\} \quad (\text{E18})$$

is the set of values x for which a match with a job of type n producing output y is viable. Using the ToL wage protocol $W_t(\phi_t^u, x, y, n) = U_t(x)$, we can rewrite the value of unemployment as:

$$rU_t(x) = Z_t^b b + \partial_t U_t \quad (\text{E19})$$

The value of an employed worker of type x paid w on a job of type (y, n) is:

$$\begin{aligned}
(r + \delta + sp_t) W_t(w, x, y, n) &= w + Z_t^x xa(n) + \underbrace{\delta U_t(x)}_{\text{exogenous layoff}} \\
&+ sp_t \sum_{y', n'} \left[\underbrace{\mathbb{I}_{\{(y', n') \in \mathcal{Q}_t(x, y, n)\}} W_t(\phi_t^q, x, y', n')}_{\text{worker quits to better job}} \right. \\
&+ \underbrace{\mathbb{I}_{\{(y', n') \in \mathcal{R}_t(x, y, n)\}} W_t(\phi_t^r, x, y, n)}_{\text{worker is retained with higher wage}} \\
&+ \underbrace{\mathbb{I}_{\{(y', n') \in \mathcal{N}_t(x, y, n)\}} W_t(w_t, x, y, n)}_{\text{worker meets worse job}} \left. \right] \left(\frac{v_t(n')}{v_t} \right) f(y') \\
&+ \underbrace{\lambda \Delta_{S_t} \cdot \Delta_{W_t}}_{\text{job upgrades}} \\
&+ \partial_t W_t(w, x, y, n)
\end{aligned} \tag{E20}$$

D.4 Surplus Representation

The wage setting protocol, described in the previous section, implies the following relationships between ϕ^q , ϕ^r , and the value functions:

$$\begin{aligned}
W_t(\phi_t^q, x, y', n') &= S_t(x, y, n) - \tilde{\Omega}_t(n) + U_t(x) \\
W_t(\phi_t^r, x, y, n) &= S_t(x, y', n') - \Omega_t(n') + U_t(x) \\
J_t(\phi_t^r, x, y, n) &= S_t(x, y, n) - [S_t(x, y', n') - \Omega_t(n')]
\end{aligned}$$

We can use these relationships to rewrite the Bellman equations for the worker and the firm as follows:

$$\begin{aligned}
(r + \delta + sp_t) W_t(w, x, y, n) &= w + Z_t^x xa(n) + \delta U_t(x) \\
&+ sp_t \sum_{(y', n') \in \mathcal{Q}_t(x, y, n)} [S_t(x, y, n) - \tilde{\Omega}_t(n) + U_t(x)] f(y') \left(\frac{v_t(n')}{v_t} \right) \\
&+ sp_t \sum_{(y', n') \in \mathcal{R}_t(x, y, n)} [S_t(x, y', n') - \Omega_t(n') + U_t(x)] f(y') \left(\frac{v_t(n')}{v_t} \right) \\
&+ sp_t \sum_{(n', y') \in \mathcal{N}_t(x, y, n)} W_t(w, x, y, n) \left(\frac{v_t(n')}{v_t} \right) f(y') \\
&+ \lambda \Delta_{S_t} \cdot \Delta_{W_t} \\
&+ \partial_t W_t(w, x, y, n)
\end{aligned}$$

$$\begin{aligned}
(r + \delta + sp_t)J_t(w, x, y, n) &= y_t - w + \delta\tilde{\Omega}_t(n) \\
&+ sp_t \sum_{(n', y') \in Q_t(x, y, n)} \tilde{\Omega}_t(n) \cdot f(y') \left(\frac{v_t(n')}{v_t} \right) \\
&+ sp_t \sum_{(n', y') \in \mathcal{R}_t(x, y, n)} [S_t(x, y, n) - S_t(x, y', n') + \Omega_t(n')] f(y') \left(\frac{v_t(n')}{v_t} \right) \\
&+ sp_t \sum_{(n', y') \in \mathcal{N}_t(x, y, n)} J_t(w, x, y, n) f(y') \left(\frac{v_t(n')}{v_t} \right) \\
&+ \lambda \Delta_{S_t} (\Delta_{J_t} - \frac{1}{2} \Delta_{S_t}) \\
&+ \partial_t J_t(w, x, y, n)
\end{aligned}$$

Summing up these two equations, we get

$$\begin{aligned}
(r + \delta + sp_t)(J_t + W_t) &= y_t + Z_t^x xa(n) + \delta [U_t(x) + \tilde{\Omega}_t(n)] \\
&+ sp_t \sum_{(y', n') \in Q_t(x, y, n)} [S_t(x, y, n) + U_t(x)] f(y') \left(\frac{v_t(n')}{v_t} \right) \\
&+ sp_t \sum_{(n', y') \in \mathcal{R}_t(x, y, n)} [S_t(x, y, n) + U_t(x)] f(y') \left(\frac{v_t(n')}{v_t} \right) \\
&+ sp_t \sum_{(n', y') \in \mathcal{N}_t(x, y, n)} [S_t(x, y, n) + U_t(x)] f(y') \left(\frac{v_t(n')}{v_t} \right) \\
&+ \frac{\lambda}{2} \Delta_{S_t}^2 \\
&+ \partial_t (J_t + W_t)
\end{aligned}$$

Subtracting the value of unemployment (E19) from both sides and simplifying yields

$$\begin{aligned}
(r + \delta + sp_t)(J_t + W_t - U_t) &= Z_t^y y + Z_t^x xa(n) - Z_t^b b + \delta [U_t(x) + \tilde{\Omega}_t(n)] - \delta U_t(x) \\
&+ sp_t \sum_{(y', n') \in Q_t(x, y, n)} [S_t(x, y, n)] f(y') \left(\frac{v_t(n')}{v_t} \right) \\
&+ sp_t \sum_{(n', y') \in \mathcal{R}_t(x, y, n)} [S_t(x, y, n)] f(y') \left(\frac{v_t(n')}{v_t} \right) \\
&+ sp_t \sum_{(n', y') \in \mathcal{N}_t(x, y, n)} [S_t(x, y, n)] f(y') \left(\frac{v_t(n')}{v_t} \right) \\
&+ \frac{\lambda}{2} \Delta_{S_t}^2 \\
&+ \partial_t (J_t + W_t - U_t)
\end{aligned}$$

and thus, recalling that $S_t = J_t + W_t - U_t$, we obtain the final expression for the surplus in the

main text

$$(r + \delta)S_t(x, y, n) = Z_t^y y + Z_t^x x a(n) - Z_t^b b + \mathbb{I}_{\{n=1\}} \frac{\lambda}{2} (S(x, y, 2) - S(x, y, 1))^2 \\ + \delta \tilde{\Omega}_t(n) + \partial_t S_t(x, y, n)$$

subject to the boundary condition $S_t(x, y, n) \geq \tilde{\Omega}_t(n)$. We note that the model is not block-recursive as in [Lise and Robin \(2017\)](#) because the firm outside option $\tilde{\Omega}_t$ is not zero, and it depends on equilibrium distributions as we show in the next section.

D.5 Value of Active and Dormant Vacancies

As outlined in the main text, vacancies enter the vacancy pool and at some rate meet a worker of type x . Upon drawing the idiosyncratic value y , it is determined whether the match is viable and a match of type (x, y, n) starts producing. If the vacant position does not meet a viable worker, it remains vacant. A vacant job is destroyed exogenously at rate δ_v . In addition, an actively recruiting vacancy of type $n = 1$ has the opportunity to upgrade at rate $\vartheta\pi$, whereas dormant vacancies cannot upgrade.

The value of an actively recruiting vacancy $\Omega_t(n)$ is given by

$$(r + q_t + \delta_v) \Omega_t(n) = q_t \sum_{x, y} \left[\mathbb{I}_{\{x \in \mathcal{H}_t(y, n)\}} J_t(\phi_t^u, x, y, n) \left(\frac{u_t(x)}{\mathbf{s}_t} \right) \right. \\ + \mathbb{I}_{\{x \notin \mathcal{H}_t(y, n)\}} \Omega_t(n) \left(\frac{u_t(x)}{\mathbf{s}_t} \right) \\ + \sum_{y', n'} \mathbb{I}_{\{(x, y', n') \in \mathcal{P}_t(y, n)\}} J_t(\phi_t^q, x, y, n) \left(\frac{s \cdot e_t(x, y', n')}{\mathbf{s}_t} \right) \\ + \sum_{y', n'} \mathbb{I}_{\{(x, y', n') \notin \mathcal{P}_t(y, n)\}} \Omega_t(n) \left(\frac{s \cdot e_t(x, y', n')}{\mathbf{s}_t} \right) \left. \right] f(y) \\ + \frac{\vartheta\lambda}{2} \Delta_{\Omega_t}^2 \\ + \partial_t \Omega_t(n)$$

The hiring set $\mathcal{H}_t(y, n)$ is defined in equation [\(E18\)](#). The poaching set

$$\mathcal{P}_t(y, n) = \{(x, y', n') : S_t(x, y, n) - \Omega_t(n) > S_t(x, y', n') - \tilde{\Omega}_t(n')\} \quad (\text{E22})$$

contains all workers of type x employed on jobs of type (y', n') that can be successfully poached by a firm of type (y, n) at date t . $S_t(x, y, n) - \Omega_t(n)$ is the net surplus of the vacant job and $S_t(x, y', n') - \tilde{\Omega}_t(n')$ is the net surplus of the competing firm.

To solve the model, it is useful to simplify this expression further, such that it does not depend on wage functions ϕ . To do so, we can substitute in

$$J_t(\phi_t^u, x, y, n) = S_t(x, y, n) \quad (\text{E23})$$

$$J_t(\phi_t^q, x, y, n) = S_t(x, y, n) - S_t(x, y', n') + \tilde{\Omega}_t(a') \quad (\text{E24})$$

This yields

$$\begin{aligned} (r + q_t + \delta_v) \Omega_t(n) = & q_t \sum_{x,y} \left[\mathbb{I}_{\{x \in \mathcal{H}_t(y,n)\}} S_t(x, y, n) \left(\frac{u_t(x)}{s_t} \right) \right. \\ & + \mathbb{I}_{\{x \notin \mathcal{H}_t(y,n)\}} \Omega_t(n) \left(\frac{u_t(x)}{s_t} \right) \\ & + \sum_{y',n'} \mathbb{I}_{\{(x,y',n') \in \mathcal{P}_t(y,n)\}} [S_t(x, y, n) - S_t(x, y', n') + \tilde{\Omega}_t(a')] \left(\frac{s \cdot e_t(x, y', n')}{s_t} \right) \\ & + \sum_{y',n'} \mathbb{I}_{\{(x,y',n') \notin \mathcal{P}_t(y,n)\}} \Omega_t(n) \left(\frac{s \cdot e_t(x, y', n')}{s_t} \right) \Big] f(y) \\ & + \frac{\vartheta \lambda}{2} \Delta_{\Omega_t}^2 \\ & + \partial_t \Omega_t(n) \end{aligned}$$

which, using the set definitions from above, corresponds to the following equation:

$$\begin{aligned} (r + \delta_v + q_t) \Omega_t(n) = & q_t \sum_{x,y} f(y) \cdot \left[\left(\max\{\Omega_t(n), S_t(x, y, n)\} \cdot \frac{u_t(x)}{s_t} \right) \right. \\ & + \left(\sum_{y',n'} \max\{\Omega_t(n), S_t(x, y, n) - S_t(x, y', n') + \tilde{\Omega}_t(a')\} \cdot \frac{s_e \cdot e_t(x, y', n')}{s_t} \right) \Big] \\ & + \frac{\vartheta \lambda}{2} \Delta_{\Omega_t}^2 + \partial_t \Omega_t(n) \end{aligned} \quad (\text{E25})$$

Finally, the value of a dormant vacancy of type n , $\tilde{\Omega}_t(n)$, is simply given by

$$(r + \delta_v + \mu) \tilde{\Omega}_t(n) = \mu \Omega_t(n) + \partial_t \tilde{\Omega}_t(n) \quad (\text{E26})$$

D.6 Labor Market Flows

It is useful to write explicitly the dynamic equations for unemployment, employment, and vacancies. The law of motion for the unemployed is

$$\begin{aligned}
 du_t(x) = & \underbrace{\delta \sum_{n,y} \mathbb{I}_{\{S_t(x,y,n) > \tilde{\Omega}(n)\}} e_t(x,y,n) dt}_{\text{exogenous EU}} + \underbrace{\sum_{n,y} \mathbb{I}_{\{S_t(x,y,n) = \tilde{\Omega}(n)\}} e_t(x,y,n)}_{\text{endogenous EU}} \\
 & - \underbrace{p_t u_t(x) \sum_{y,n} \mathbb{I}_{\{x \in \mathcal{H}_t(y,n)\}} \left(\frac{v_t(n)}{\mathbf{v}_t} \right) f(y) dt}_{\text{hires from unemployment}}
 \end{aligned} \tag{E27}$$

where du_t denotes the change in u in a small time interval from t to $t + dt$.

For the employed,

$$\begin{aligned}
 de_t(x,y,n) = & \underbrace{-\delta \mathbb{I}_{\{S_t(x,y,n) > \tilde{\Omega}_t(n)\}} e_t(x,y,n) dt}_{\text{exogenous EU}} - \underbrace{\mathbb{I}_{\{S_t(x,y,n) = \tilde{\Omega}_t(n)\}} e_t(x,y,n)}_{\text{endogenous EU}} \\
 & - \underbrace{sp_t e_t(x,y,n) \left[\sum_{y',n'} \mathbb{I}_{\{(y',n') \in \mathcal{Q}_t(x,y,n)\}} \left(\frac{v_t(n')}{\mathbf{v}_t} \right) f(y') \right] dt}_{\text{EE outflow}} \\
 & + \underbrace{sp_t \sum_{y',n'} e(x,y',n') \mathbb{I}_{\{(x,y',n') \in \mathcal{P}_t(y,n)\}} \left(\frac{v_t(n)}{\mathbf{v}_t} \right) f(y) dt}_{\text{EE inflow}} \\
 & + \underbrace{p_t u_t(x) \mathbb{I}_{\{x \in \mathcal{H}_t(y,n)\}} \left(\frac{v_t(n)}{\mathbf{v}_t} \right) f(y) dt}_{\text{UE hires}} \\
 & + \underbrace{(\mathbb{I}_{\{n=2\}} - \mathbb{I}_{\{n=1\}}) \lambda \Delta s e_t(x,y,1) dt}_{\text{upgrades}}
 \end{aligned} \tag{E28}$$

For active vacancies,

$$\begin{aligned}
dv_t(n) = & \underbrace{-\delta_v v_t(n) dt}_{\text{vac. destruction}} + \underbrace{i_t(n) dt}_{\text{vac. creation}} + \underbrace{\mu \tilde{v}(n) dt}_{\text{entry from dormant}} + \underbrace{(\mathbb{I}_{\{n=2\}} - \mathbb{I}_{\{n=1\}}) \lambda \theta \Delta_{\Omega_t} v_t(1) dt}_{\text{upgrades}} \\
& - q_t v_t(n) \sum_{x,y} \underbrace{\mathbb{I}_{\{x \in \mathcal{H}_t(y,n)\}} \left(\frac{u_t(x)}{s_t} \right)}_{\text{vacancies filled from } u} \\
& + \underbrace{\sum_{y',n'} \mathbb{I}_{\{(x,y',n') \in \mathcal{P}_t(y,n)\}} \left(\frac{s \cdot e_t(x,y',n')}{s_t} \right)}_{\text{vacancies filled from } e} \Bigg] f(y) dt
\end{aligned} \tag{E29}$$

For dormant vacancies,

$$\begin{aligned}
d\tilde{v}_t(n) = & \underbrace{-\delta_v \tilde{v}_t(n) dt}_{\text{vac. destruction}} - \underbrace{\mu \tilde{v}_t(n) dt}_{\text{exit from dormant}} \\
& + \sum_{x,y} \left[\underbrace{\delta \mathbb{I}_{\{S_t(x,y,n) > \bar{\Omega}_t(n)\}} e_t(x,y,n) dt}_{\text{exogenous EU}} + \underbrace{\mathbb{I}_{\{S_t(x,y,n) = \bar{\Omega}_t(n)\}} e_t(x,y,n)}_{\text{endogenous EU}} \right. \\
& \left. + \underbrace{sp_t e_t(x,y,n) \sum_{y',n'} \mathbb{I}_{\{(y',n') \in \mathcal{Q}_t(x,y,n)\}} \left(\frac{v_t(n')}{v_t} \right) f(y') dt}_{\text{EE outflow}} \right]
\end{aligned} \tag{E30}$$

D.7 Match Efficiency

Match efficiency in our model is endogenous. It is given by the ratio of hires to contacts. This ratio depends on contact rates and match formation decisions. Let A_t^u and A_t^e denote match efficiency for the employed and the unemployed, respectively. It is easy to derive that, in our model:

$$A_t^u = \frac{UE_t}{p_t u_t} = \sum_{x,y,n} \mathbb{I}_{\{x \in \mathcal{H}_t(y,n)\}} \left(\frac{u_t(x)}{u_t} \right) \left(\frac{v_t(n)}{v_t} \right) f(y) \tag{E31}$$

$$A_t^e = \frac{EE_t}{p_t s e_t} = \sum_{x,y,n} \left[\sum_{y',n'} \mathbb{I}_{\{(x,y',n') \in \mathcal{P}_t(y,n)\}} \frac{e_t(x,y',n')}{e_t} \right] \left(\frac{v_t(n)}{v_t} \right) f(y) \tag{E32}$$

Aggregate match efficiency is given by the average between the two weighted by the share of unemployed and employed job seekers, respectively.

$$A_t = A_t^u \frac{u_t}{u_t + s e_t} + A_t^e \frac{s e_t}{u_t + s e_t} \tag{E33}$$

D.8 Equilibrium

Given initial distributions $u_0(x), e_0(x, y, n), v_0(n), \tilde{v}_0(n)$ and paths for the aggregate shocks $\{Z_t^x, Z_t^y, Z_t^b\}_{t \geq 0}$, a *perfect foresight equilibrium* in this economy is

1. A list of value functions $\{S_t(x, y, n), J_t(w, x, y, n), U_t(x), W_t(w, x, y, n), \Omega_t(n), \tilde{\Omega}_t(n)\}_{t \geq 0}$ that satisfy equations (10), (E14), (E19), (E20), (E21), and (E26)
2. Quit, retention and neutral sets, $\{Q_t(x, y, n), \mathcal{R}_t(x, y, n), \mathcal{N}_t(x, y, n)\}_{t \geq 0}$ that satisfy equations (E15), (E16), (E17); Hiring and poaching sets $\{\mathcal{H}_t(y, n), \mathcal{P}_t(y, n)\}_{t \geq 0}$ that satisfy equations (E18), and (E22); Upgrading sets $\{\mathcal{U}_S(x, y), \mathcal{U}_\Omega\}_{t \geq 0}$ that satisfy equations (E12) and (E13)
3. Distributions $\{u_t(x), e_t(x, y, n), v_t(n), \tilde{v}_t(n)\}_{t \geq 0}$ that satisfy the laws of motion in equations (E27), (E28), (E29), and (E30), and implied meetings $m_t = m(v_t, s_t)$
4. Hiring, poaching, retention, and upgrading wage functions $\{\phi_t^u(x, y, n), \phi_t^q(x, y, y', n, n'), \phi_t^r(x, y, y', n, n'), \phi_t^\dagger(x, y, n)\}_{t \geq 0}$ defined in equations (E1), (E3), (E5), and (E11), and boundary wage functions $\{\phi_t^+(x, y, n), \phi_t^-(x, y, n)\}_{t \geq 0}$ defined in equations (E7) and (E9)
5. A measure of entrants $i_t(n)$ that satisfies the free entry condition in equation (8)

D.9 Solving the Model

Taking stock, we can now construct a solution algorithm for the model, using the equations in the previous subsections.

We begin from the stationary equilibrium, a special case of the definition of Section D.8 where all aggregate shocks are constant forever. We denote by $*$ quantities and values in steady state. For example, steady-state surplus is

$$S^*(x, y, n) = y + xa(n) - b + \frac{\lambda}{2} \Delta_{S^*}^2 + \delta \tilde{\Omega}^*$$

i.e., in equation (10) we omit the time dependence and set the term involving ∂_t to zero. And similarly for all other values. Steady-state unemployment is computed from (E27) by setting $du_t/dt = 0$ and dropping t subscripts from all terms in that law of motion. And similarly for all other stocks. To compute the *stationary equilibrium*:

1. Guess a value for $\Omega^*(n)$.
2. Compute S^* and $\tilde{\Omega}^*$ conditional on the guess for Ω^* using equations (10) and (E26) evaluated at steady state.

3. Compute all distributions $u^*(x), e^*(x, y, n), v^*(n), \tilde{v}^*(n)$ conditional on $\Omega^*, \tilde{\Omega}^*, S^*$, using the laws of motion (E27), (E28), (E29), and (E30) evaluated at steady state.
4. Update $\Omega^*(n)$ to reduce the error in equation (E25).
5. Iterate until equation (E25) evaluated at steady state holds. These steps allow to compute all steady-state quantities.
6. Compute U^*, W^*, J^* and solve for all wages through equations (E1), (E3), (E5), (E11), (E7) and (E9) evaluated at steady state.

We now turn to the calculation of a perfect foresight equilibrium. Suppose we have a set of initial conditions for our distributions $\{u_0(x), e_0(x, y, n), v_0(n), \tilde{v}_0(n)\}$, and a sequence of realizations of aggregate shocks $\{Z_t^x, Z_t^y, Z_t^b\}_{t=0}^T$ in hand. Suppose at $t = T$ the economy is back to steady state, and we have already computed all the stationary equilibrium objects. To compute the *perfect foresight equilibrium*:

1. Guess a sequence $\{\Omega_t(n)\}_{t=0}^T$.
2. Through backward iteration, starting at $t = T$, compute S_t and $\tilde{\Omega}_t$ conditional on the guess for Ω_t using equations (10) and (E26).
3. Through forward iteration, compute all distributions $u_t(x), e_t(x, y, n), v_t(n), \tilde{v}_t(n)$ conditional on $\Omega_t, \tilde{\Omega}_t, S_t$, using the laws of motion (E27), (E28), (E29), and (E30).
4. Update $\Omega_t(n)$ to reduce the error in equation (E25).
5. Iterate until equation (E25) holds. These steps allow to compute all equilibrium allocations at every t .
6. To obtain wages, compute first $\{U_t, W_t, J_t\}$ and next solve for all wages through equations (E1), (E3), (E5), (E11), (E7) and (E9).

E Additional Model Figures

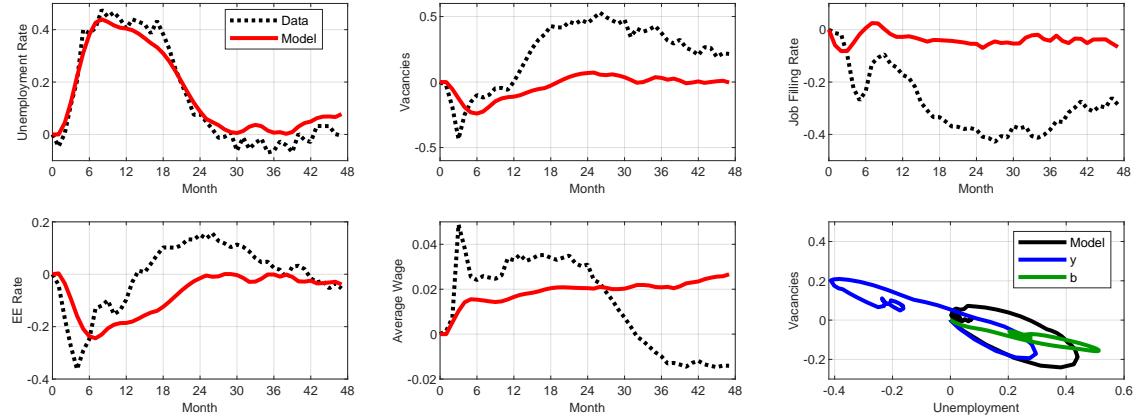


Figure E1: Model-simulation keeping the job amenity value fixed at its initial steady state. Bottom right panel: Model's Beveridge curve (black) and decomposition into dynamics induced by productivity (blue) and opportunity cost of work (green) shocks. Other panels: Model's fit of the data. Data in black dashed line and model in solid red line. Log-deviations from initial steady state.

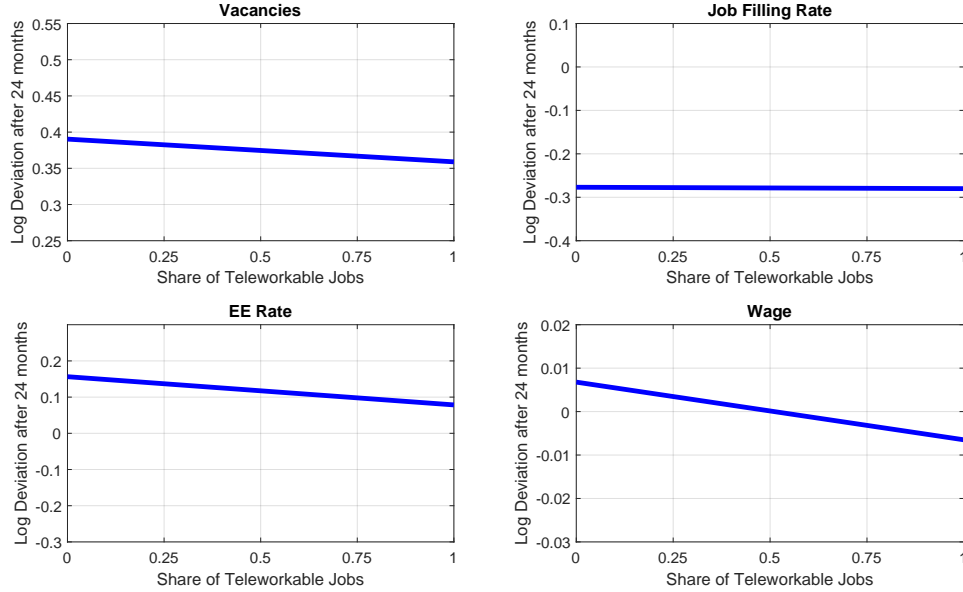


Figure E2: Model counterpart of the cross-sectoral evidence of Figure 8 under a shock to the speed of upgrading λ . The scale is the same as the one in Figure 18 to facilitate the comparison.